Universität für Bodenkultur Wien

University of Natural Resources and Life Sciences, Vienna

Department of Civil Engineering and Natural Hazards,

Institute of Mountain Risk Engineering

Master thesis

Forest Effects on Avalanche Dynamics: Evaluation and Improvement of the Avalanche Model RAMMS

Natalie Brožová MSc.

Supervised by:

Dr. Peter Bebi, SLF Davos

Dipl.-Phys. Dr.techn. Jan-Thomas Fischer, BFW Innsbruck

Univ.Prof. Dipl.-Ing. Dr.nat.techn. Johannes Hübl, IAN BOKU Wien

Innsbruck, 2018

BOKU Institut für Alpine Naturgefahren (IAN)

WSL Institute for Snow and Avalanche Research SLF

BFW Bundesforschungszentrum für Wald

Acknowledgments

I would like to express my thankfulness to people, who made my work possible. I would especially like to thank Peter Bebi from SLF who inspired me for this study field already before we met. He guided me from the beginning to the end of my work and always supported me with valuable knowledge and encouragement. It was a great pleasure to work with him and I was glad to be able to discuss any problem that occurred. I thank other advisors from SLF as Perry Bartelt, who helped me a lot with the RAMMS simulations and brought his different perspective to my research, as well as Yves Bühler and Marc Christen. It was an incredible experience in my life being able to stay in Davos and I would like to thank to all my friends and colleagues that I met there, for spending the time with me, especially to Nathan, Gianna and Eddie.

Thanks to Jan-Thomas Fischer for helping me to establish the connections in the beginning and to bring my work to a finish at BFW, for all corrections and constructive comments and critic. Thanks to my BFW colleagues for creating nice working atmosphere.

Thanks to all my other friends, colleagues, my family and Giacomo for their support.

Abstract

Mountain forests offer effective, natural and cost-efficient protection against avalanches. Slowing and stopping behaviour of small avalanches within a forest has been observed. To simulate the forest influence on the avalanche dynamics, the scientific version of the simulation tool RAMMS calculates frictional effects as well as detrainment effects of the trees. The second role that forest plays in the avalanche mitigation is the reduction of the potential avalanche formation and release. The influence of a mature forest is well documented; however, the effect of initial stages of forest succession and shrub vegetation is less clear.

To address the first issue, I tested three remote sensing methods together with forest information obtained in the field. Forest parameters, such as maximal tree height, surface roughness, diameter at breast height (DBH), resulting detrainment coefficients (K-values) and the simulation outputs were compared. Large database on trees and snow information at the high afforestation at Stillberg was used to test the influence of the initial stage of forest succession on avalanche formation and release.

There are slight differences in the maximal tree height depending on the forest group (dense forest, open forest and green alder) comparing the remote sensing methods and the field method. Surface roughness is underestimated using the digital terrain model in comparison to the roughness observed in the field. DBH calculated using the formula from RAMMS does not fit the data collected at Stillberg area for two of three tree species. However, the K-values do not show a major influence on the simulated runout distances and the simulation outputs did not show major differences comparing all the methods together. The current VHM available for whole Switzerland may thus have a sufficient accuracy to determine forest parameters for avalanche simulations.

Number of trees has a significant influence on the maximal snow height already after 10 years after planting. Maximal snow height decreases with an increasing number of trees per plot. Growing trees lead thus subsequently in lower maximal snow depths, increasing the snow stability and preventing avalanche releases. At the Stillberg afforested area, where the avalanches periodically released before and during the first years of the afforestation, no more avalanche activity was observed more than 36 years after the afforestation. More research in the direction of interception of the initial stages of forest succession is essential in order to further improve the quantification of critical thresholds for the prediction of avalanche formation in forested terrain.

Zusammenfassung

Bergwälder bieten effektive und ökologische Schutzwirkung gegen Lawinen. Kleine und mittelgroße Lawinen werden von Wald abgebremst oder gestoppt. In der neuen wissenschaftliche Version der Lawinensimulationssoftware RAMMS sind die Wirkungen sowohl der Bodenrauigkeit der Vegetation als auch von Schneedetrainment implementiert. Der Wald spielt zudem vor allem eine wichtige Rolle bei der Lawinenbildung, da in dichtem Wald weniger Schnee gelagert wird und auch weniger Schwachschichten gebildet werden, welche zu Schneebrettlawinen führen können. Die Schutzwirkung von Hochwald ist gut dokumentiert, die Einflüsse von junge Bäumen und Sträuchern sowie die Erfassung der Schutzwirkung mit neuen Fernerkundungsmethoden sind hingegen weniger gut bekannt. In dieser Arbeit ging ich deshalb folgenden zwei Fragen nach: 1) Wie lassen sich neue Fernerkundungsmethoden für die Verwendung von Lawinensimulationen mit Waldintersektion einsetzen; und 2) Wie hat sich die Lawinenschutzwirkung von Jungbäumen in der Hochlagenaufforstung Stillberg im Laufe der letzten 40 Jahren verändert?

Die durch Fernerkundungsmethoden ermittelten Waldparameter (maximale Baumhöhe, Brusthöhendurchmesser (BHD) und Bodenrauigkeit) wurden mit Felddaten dieser Parameter verglichen. Durch Implementierung dieser Parameter in das Lawinensimulationsprogramm RAMMS wurden daraus auch Unterschiede bezüglich Schneedetrainment (K-Werte) und Lawinenauslauflänge abgeleitet.

In Abhängig vom Waldtyp (dichter Wald, offener Wald und Grünerle) gab es nur leichte Unterschiede zwischen verschiedenen Messmethoden bezüglich der maximalen Baumhöhe. Die Bodenrauigkeit wurde jedoch mittels Bestimmung durch digitalen Geländemodelle im Vergleich zu den Feldbeobachtungen unterschätzt. Der berechneter BHD entspricht nicht die BHD-Höhenkurve von im Feld erhobenen Daten am Stillberg für zwei von drei Baumarten. Die K-Werte im untersuchten Bereich haben nur wenig Einfluss auf die Lawinenauslauflängen, und die Lawinensimulationsresultate zeigen keine größeren Unterschiede zwischen den Fernerkundungsmethoden und der Feldmethode. Das aktuelle Vegetationshöhenmodell der Schweiz scheint daher geeignet zu sein für großflächige Abschätzung von Waldparametern für Lawinensimulation.

Der Anzahl der Bäume auf der Stillberg-Versuchsfläche hatte schon nach 10 Jahren einen signifikanten Einfluss auf die maximalen Schneehöhen. Je mehr Bäume pro Stichprobe vorhanden waren, desto niedriger war die Schneehöhe. Der junge Wald am Stillberg hatte schon 36 Jahre nach der Aufforstung Anrisse von weiteren Lawinen verhindern. Für eine noch bessere Abschätzung der Lawinenschutzwirkung in Anrissgebieten, wäre es wertvoll, die Interzeption von Schnee in verschiedenen Sukzessionsstadien noch besser zu quantifizieren.

Contents

1 Introduction

Snow avalanches next to rockfall, landslides, debris-flows and others are known as mountain-slope hazards, which are not included on a world scale in "big five" of natural hazards (earthquakes, floods, tropical storms, drought and volcanic hazards) affecting large areas with high damage costs. However, snow avalanches are continuous with fatalities every winter in most snow-covered mountain areas of the world (McClung and Schaerer, 2006; Figure 1).

To reduce the avalanche risk, temporal and permanent mitigation measures are used (McClung and Schaerer, 2006, Schweizer et al., 2015). The oldest active mitigation measure is protection forest, which is natural, effective and efficient instrument against natural hazards. Protection forest plays several roles in mitigating the avalanche releases. Forest influences the structure of snowpack and thereby the avalanche activity through interception, microclimate and higher surface roughness caused by the trees, stumps and lying dead wood (Schneebeli and Bebi, 2004; Bebi et al, 2009a; Teich et al., 2012a). Less investigated effect of forests on avalanches is the capacity of stopping or slowing avalanches in the forest stand. This ability is however limited, and large, fast moving avalanches destroy the forest. Recording forest damage and destruction can be useful for characterisation of the avalanche patterns as intensity or return periods (Feistl et al., 2015). The forest is able to stop small to medium size avalanches, which are crucial for road and ski-run safety (Feistl et al. 2014).

One of the most important planning tools in the Alpine regions is the hazard zone mapping. Information for creating such hazard maps are taken from documented events, but also from natural hazard simulations. While traditional avalanche simulation tools have included forest only as a factor of surface roughness, a later version of the avalanche simulation tool RAMMS (Rapid Mass Movement Simulation) considers also the deposition of snow behind trees and the subsequent effect on the energy and the runout length of an avalanche (Teich, 2013; Feistl, 2015). Simulation of small to medium size avalanches have thus been improved by including the detrainment coefficient K which accounts for the effect of the forest cover and varies according to forest type and canopy closure, vertical structure and surface cover (Teich et al., 2014). It is fundamental to gather forest parameters before initiating of simulation; this is nowadays mostly done from remote sensing data, which is likely the

most efficient and accurate method for quantifying forest biomass on a large scale. However, it is not clear, if remote sensing data (e.g. orthophoto, digital surface and terrain models, vegetation height model and other digital data) are able to deliver the necessary inputs on forest characteristics to simulate precise output. To validate the remote sensing data, I will proceed with fieldwork verification to study how single forest parameters and the avalanche runout distance differ.

The effect of mature forest on potential avalanche formation and propagation is relatively well documented (Bebi et al., 2009a; Teich, 2013), however the initial stages of forest succession on avalanche formation is less clear, depending on different parameters as snow cover, snow properties and topography (Frey, 1977). Different authors have published the thresholds of minimal tree heights relative to the maximum possible snow height in specific regions, which correspond to an exceeding of the maximum snow depth by a factor of 1.5-2 (Frey, 1977; McClung, 2001; Saeki and Matsuoka, 1969). In order to further improve our understanding of avalanche-forest interactions and of avalanche simulation models in forested terrain, it is thus necessary to analyse in particular interactions between avalanches and initial stages of forest succession. To proceed with the analysis, systematic afforestation at Stillberg will be used as study area thanks to large database on snow and tree data.

1.1 Research Questions

RQ1: How does the simulated avalanche runout change with changing release area and forest structure parameter (K-value) and what is the optimal method to determine it?

RQ2: How suitable are lately available remote sensing methods for the estimation of forest parameters (maximum height, DBH, K-value, terrain roughness)?

What is the difference between simulation outputs using fieldwork and remote sensing data? Is using remote sensing data reliable and the accuracy appropriate for avalanche simulation?

RQ3: How did the frequency of avalanches in the systematically afforested release area Stillberg change as a function of the spatiotemporal survival pattern of young trees and as a function of increasing tree height and increasing snow interception capacity?

2 Background

2.1 Snow avalanches

Snow avalanches are one of the most frequent hazards in the mountain areas during the winter season. They are rapid and gravity driven, meteorologically caused hazards. Thanks to the possibility of forecasting and extensive mitigation measures, avalanche fatalities on roads and houses decreased during the twentieth century (Figure 1). The most of the fatalities in Switzerland over the last 20 years involve recreational winter sport activities in the uncontrolled avalanche terrain (Techel and Zweifel, 2013).

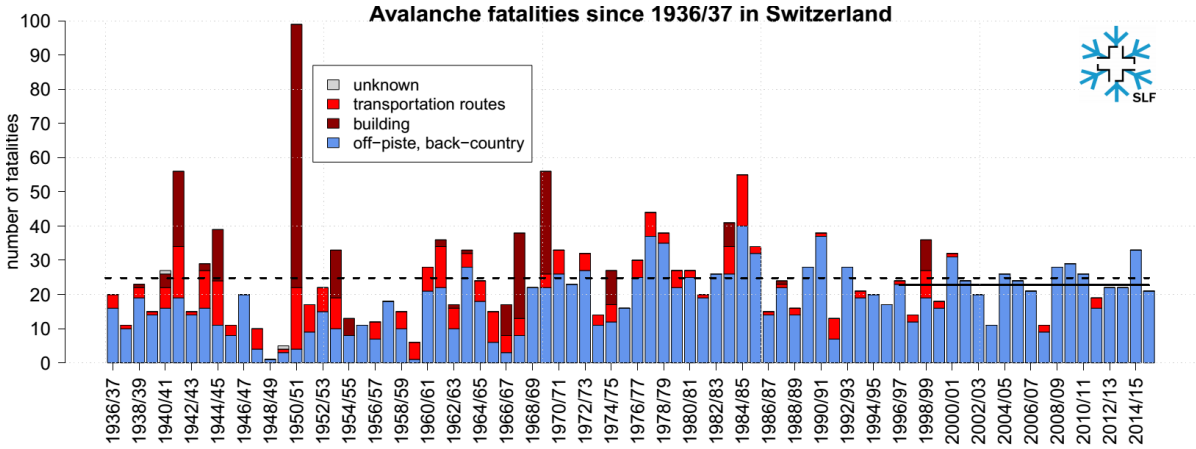

Figure 1: Avalanche fatalities in Switzerland since 1936/37. The graph illustrates the decrease in the number of fatalities in buildings and on transportation routes. It also shows the averages for the last 80 years (25; black broken line) and 20 years (23; black solid line). During the last 20 years, more than 90% of the avalanche victims lost their lives in open terrain (SLF).

2.2 Types of avalanches

The two general types of avalanches differ according to the release, they are called loose snow avalanches and slab avalanches. Loose snow avalanches originate from a point or small area at or near the surface and they usually involve only surface or near-surface layer of either dry or wet snow. The initial failure comes from the single point, spread out as the snow moves down, and entrains additional snow. The form of this avalanche type has a triangular pattern. These avalanches are rather small and less dangerous, since only the cohesionless surface layer is involved (McClung and Schaerer, 2006, Schweizer et al., 2003; Schweizer et al., 2015).

Snow slab avalanches are usually more dangerous and they represent the vast majority of fatal avalanches, because they involve generally more snow and are harder to predict (Schweizer et al., 2003; McClung and Schaerer, 2006; Schweizer et al., 2015). Three different types of slab avalanches are distinguished according to process leading to slab release: dry-snow, wet-snow and glide snow avalanches (Schweizer et al., 2015). The origin of the first two types of slab avalanches is in the weak layer, where the first failure occurs and results to a block of snow that is cut off above the crown. Slab avalanche slide on the bed surface, which can be an older snow layer or ground. The weak layer is just between the slab and the bed surface. The right and left sides of the slab are called flanks and the fractures at the flanks are caused by downslope motion. Stauchwall is the wedge-shaped lowest downslope fracture surface forming at about the same time as flanks (Schweizer et al., 2003; McClung and Schaerer, 2006; Schweizer et al., 2015).

2.3 Avalanche modelling and simulation

How to deal with the avalanche risk has been a question since people live in the mountainous areas. The main aim has always been the same, from preventing the avalanches to release in the starting zone, through changing its direction, to avoiding the exposure in the runout zones (Bründl and Margreth, 2015). Firstly, it is necessary to understand the dynamics of avalanches, which is very complex and it is difficult to include all the data to models. Several approaches are used in avalanche modeling, as the statistical approach or the fluid-mechanics approach (Ancey, 2008).

Statistical models come from the historical data on the avalanche path observations and from the methods calculating the runout distance. They are important in predicting the extension of the long-return period avalanche for a given avalanche path and they serve for risk assessment and mitigation. These models are based on topographic characteristics, which correlate with the runout distance. The longitudinal profile of the avalanche path controls the avalanche runout. Three main points on the one dimensional avalanche path include release zone, point of deceleration (where the slope is usually equal to 10°) and the stopping position (Figure 2). The α measures the average angle from the top of the avalanche path to the observed maximum runout and the β is the average angle of the avalanche path between the release point and the point

of deceleration point (McClung and Lied, 1987; Ancey, 2008; Sinickas and Jamieson, 2014).

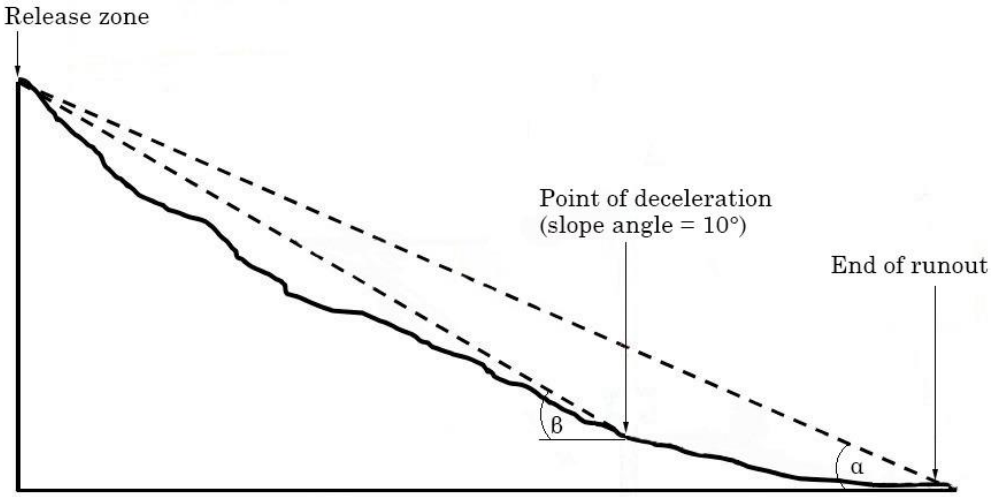

Figure 2: Longitudinal profile of avalanche path with three main points: release zone (starting point), point of deceleration (slope angle is usually equal to 10°) and the end of runout (α point). *The α measures the average angle from the release point to the maximum runout and the β is the average angle between the release point and the deceleration point (modified after Sinickas and Jamieson, 2014).*

The models based on fluid-mechanics approach describe the internal dynamics of the moving mass from the initiation of the motion to the stopping. However, it is impossible to describe snow avalanches using only fluid-mechanics approach due to many unique characteristics as particle size and composition, initial and boundary conditions, etc. (Ancey, 2008). Runout estimates based on the dynamic models are more variable than estimates from statistical runout models, but thanks to dynamical mass movement modeling, it is possible to predict the runout distances, flow velocities and impact pressures in a three-dimensional terrain. This information serve for hazard mapping and designing new mitigation measures, as well as for back-calculating documented avalanche events (Bartelt et al., 2013) or modeling different scenarios to obtain the reliable impact pressures (Jamieson et al, 2008).

Simulation tools for natural hazards in the engineering practice are increasingly demanded for better understanding of the geophysical processes. The most common avalanche tools such as RAMMS (Christen et al., 2010), ELBA+ (Jörg et al., 2012) and SAMOS-AT (Sampl and Granig, 2009) are based on empirical procedures using topographical/statistical information and comparative models for runout distance, or they are based on dynamical mass movement modeling (Bründl and Margreth, 2015).

2.3.1 RAMMS::AVALANCHE

RAMMS (Rapid Mass Movement Simulation) is a two-dimensional tool that simulates flowing snow avalanches from release to runout in three-dimensional terrain. The basic topographic data as digital elevation model (DEM), georeferenced map and image are imported. Single or multiple release areas are imported from as shapefile or easily created within the project. Information about the release has very strong impact on the results of the simulation, so it should be well defined with reference information (Bartelt et al., 2013).

The standard version of RAMMS applies the two-parameter Voellmy-fluid friction model, which is based on Voellmy-Salm approach. The model divides the frictional resistance (S) in two parts: a dry-Coulomb basal friction, which scales with the normal stress ($\rho g U^2$) and a velocity-squared drag or viscous-turbulent friction originating above the surface.

$$S = \mu \rho H g \cos(\varphi) + \frac{\rho g U^2}{\xi} \tag{1}$$

In this formula μ is the dry-Coulomb friction, ρ the density, H the flow height, g the gravitational acceleration, φ the slope angle, U the flow velocity and ξ the viscous-turbulent friction.

The friction coefficients are influencing the behaviour of the flow, where the dry-Coulomb friction (μ) prevails when the flow is stopping and the viscous-turbulent friction (ξ) dominates during high velocity flow. These friction parameters can be included in the simulation as constant as well as variable. Variable friction parameters are based on the topographic data analysis (slope angle, altitude and curvature), forest information and global parameters (return period and avalanche volume). They strongly depend on the return period and avalanche volume (Christen et. al, 2010).

The scientific version of RAMMS uses the thermomechanical dynamics equations, which describe four physical processes: 1) The rise in avalanche temperature by frictional dissipation. 2) Phase changes and the production of meltwater. 3) Entrainment of snow mass and the associated internal (thermal) energy change of the avalanche. 4) Constitutive models describing how the avalanche flow rheology changes as a function of temperature and moisture content (Vera Valero et al., 2017).

2.4 Forest-avalanche interaction

It has been known, since people live in the mountains, that forests can provide effective protection against avalanches. Despite that the first strict regulations were created in the 14th century, it took several centuries for people to understand and accept that forest conservation and proper management were essential. Bavarian Forest Act of 1852 may represent the first recognition of the importance of protection forests and problems concerning natural hazards (Brang et al., 2001). In Switzerland, first binding regulation was the federal forest law issued in 1876 about protection and conservation of mountain forests (Leibundgut, 1978). Austria's first forest law was issued in 1852, but the term protection forest was defined in the latter forest law from 1975 (Bundesrepublik Österreich, 1975). In the case of Norway, no guidelines, legislation or regulation is to be found in the field of protection forests. Clearcutting is common and it creates new potential release areas for avalanches (Breien and Høydal, 2012).

The avalanche experts started studying the avalanche processes and the actual influence of the forests on avalanches and other ways to hinder the avalanche occurrence mostly in the second half of the twentieth century, mainly in the Alps and Rocky Mountains (Schneebelli and Bebi, 2004). One of the objectives of protection forests is reducing the potential release of the avalanche in the starting zone. The most important factor in the starting zone on forested terrain is the slope inclination typically with values between 30° to 55° (Schneebeli and Bebi, 2004; Sitko, 2008). Unlike the first one, the factor of basal friction is possible to change and it varies with different vegetation cover (Sitko, 2008; Feistl et al., 2014). Higher surface roughness, which depends on the vegetation cover, terrain irregularities as ridges and holes or with left woody debris and stumps, hinder the avalanche formation (Schneebeli and Bebi, 2004; Bebi et al, 2009a). These terrain features also support the forest regeneration by creating favourable microsites for the seedlings and hinder the damages on young trees in the form of snow gliding and creeping (Schneebeli and Bebi, 2004).

A great reduction of the slab avalanches in the forest is observed thanks to the supporting force of the stems and to the structure of the snow, which is influenced by the interception of the crowns. The interception controlling the amount of snow in forest, counts up to 70% during low snowfalls in comparison to 30% during heavy snowfalls. Reduced solar radiation during the day and long-wave radiation during the night are slighter, influencing the transformation of the snow and hindering the formation of surface and depth hoar. In contrast to open terrain, the wind under the

forest cover has less influence on the snow surface therefore less drifting snow accumulates in gullies and depressions (Bebi et al, 2009a; de Quervain, 1978; McClung and Schaerer, 2006; Schneebeli and Bebi, 2004).

As the subalpine forest is found in the high altitudes close to the mountain tops, where the conditions for growth are harsh, fewer trees are occurring and the boundary of tree growth is determined by the treeline. Above the timberline, forest density decreases and tree clusters are often formed with typical forest gaps in between (Jørgensen, 2009). These gaps are prone for the initiation of the glide-snow avalanches. Even though these avalanches are difficult to predict, it is possible to set the thresholds for different parameters to prevent the release of such avalanches. These parameters include next to the slope and the ground roughness, also height of the snow and size of the gap (Feistl et al., 2014). As more as the probability of the avalanche release is higher regarding to the topographic parameters, the forest plays more significant role in the avalanche release mitigation (Sitko, 2008).

When the release zone is above the treeline, forest cannot mitigate the initiation of an avalanche. Forest structure and composition is therefore shaped by the avalanche regime. Forest is disturbed, or in the case of smaller avalanches hinders the avalanche flow by stopping or slowing them down. Vice versa, depending on the forest structure and composition, forest has different impact on avalanches (Bebi et al., 2009a; Figure 3).

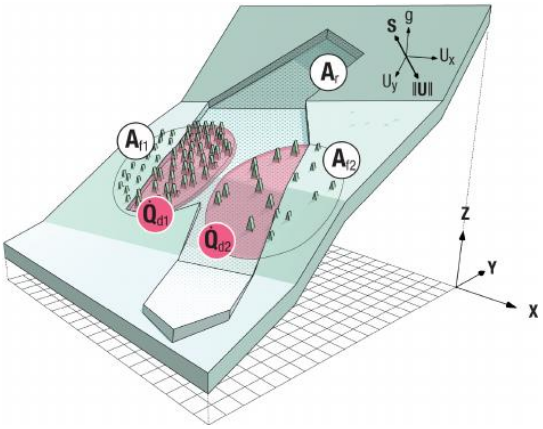

Figure 3: Schematic illustration of avalanche modeling in forested terrain. The release area (Ar) as well as forested areas (Af) have to be defined by the avalanche expert and assigned an appropriate K value dependent on specific forest characteristics which determine the detrainment rate (Qd). Avalanche flow in general is modeled by the velocities in x and y direction (Ux and Uy) and by the friction S acting in the opposite direction than |U|, and the gravitational acceleration g (Teich et al., 2014).

To evaluate the influence that forest stands with different composition and structure have of on the avalanches, it is possible to simulate the avalanche in RAMMS, where forest does not affect only the surface roughness, but also the snow detrainment (Teich, 2013; Feistl, 2015). Forest in RAMMS is classified according to forest type, crown coverage, and ground roughness that can be defined through surface cover as small vegetation, rocks, and woody debris as stumps or dead wood (Teich et al, 2014; Figure 4).

forest type	crown coverage*	roughness**	K-value***	Code
evergreen / mixed	dense (> 70%) coverage	rough (stumps/shrubs/saplings); height > 100 cm	48	A
		knobby (scree/stepped/seedlings); height 20 - 100 cm	38	B
		smooth (grass/leaves/smooth rock); height < 20 cm	28	C
	scattered, grouped (40% - 70%) coverage	rough (stumps/shrubs/saplings); height > 100 cm	43	D
		knobby (scree/stepped/seedlings); height 20 - 100 cm	33	E
		smooth (grass/leaves/smooth rock); height < 20 cm	23	F
	open (20% - 40%) coverage	rough (stumps/shrubs/saplings); height > 100 cm	38	G
		knobby (scree/stepped/seedlings); height 20 - 100 cm	28	H
		smooth (grass/leaves/smooth rock); height < 20 cm	18	I
larch / deciduous trees	dense (> 70%) coverage	rough (stumps/shrubs/saplings); height > 100 cm	35	J
		knobby (scree/stepped/seedlings); height 20 - 100 cm	25	K
		smooth (grass/leaves/smooth rock); height < 20 cm	15	L
	scattered, grouped (40% - 70%) coverage	rough (stumps/shrubs/saplings); height > 100 cm	30	M
		knobby (scree/stepped/seedlings); height 20 - 100 cm	20	N
		smooth (grass/leaves/smooth rock); height < 20 cm	10	O
	open (20% - 40%) coverage	rough (stumps/shrubs/saplings); height > 100 cm	25	P
		knobby (scree/stepped/seedlings); height 20 - 100 cm	15	Q
		smooth (grass/leaves/smooth rock); height < 20 cm	5	R

* Can be determined analysing orthophotos. Pictures below show example cases.

** Quantity for ground roughness as well as small vegetation and dead wood in the avalanche path. Examples below.

*** K in [Pa] represents the braking power per square meter that the forest exerts on the avalanche flow. It can be chosen manually if forest structure is not clear or in between two classes.

Crown coverage:

dense

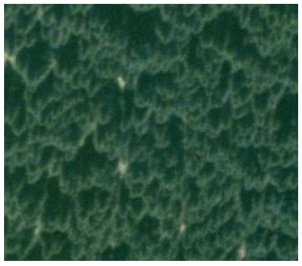

scattered, grouped

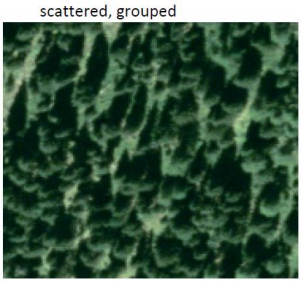

open

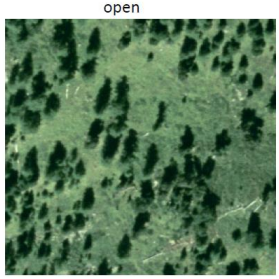

Roughness:

rough

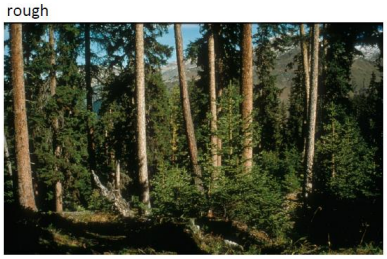

knobby

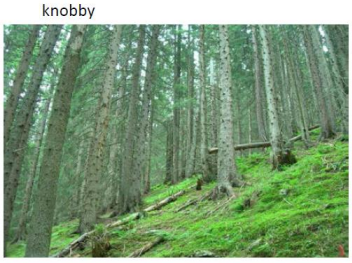

smooth

Features of ground roughness should be present every few meters. If there are only few large obstacles the roughness can be classified as knobby.

Figure 4: Look-up table of K-values for forest shape files (RAMMS).

3 Materials and Methods

3.1 Study area – Dischmatal

The study area of this research is in Dischmatal close to Davos (Graubünden, Switzerland, Figure 5). We chose two different areas on the same NE slope of Dischmatal. To address the first and the second research question, the avalanche track above Teufi was observed. Thanks to the long-term monitoring at the Stillberg afforestation, this area provides suitable conditions to answer the third research question.

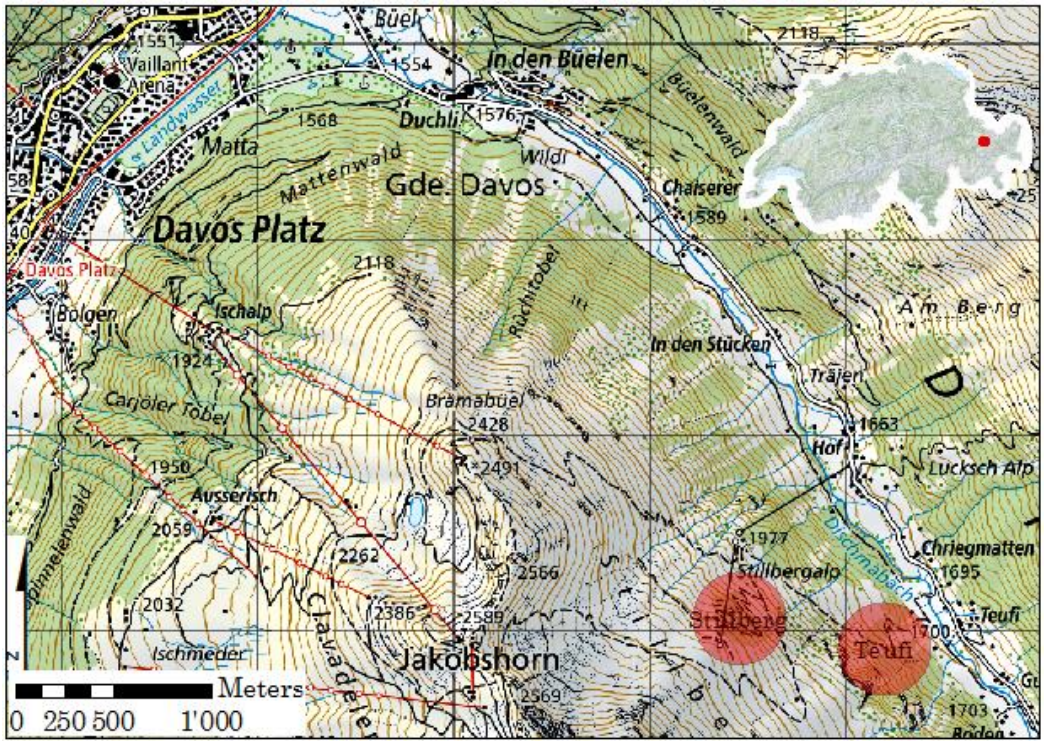

Figure 5: Study areas in Dischmatal close to Davos – Teufi and Stillberg.

3.1.1 Stillberg

Stillberg afforestation is a unique experimental area in the world, where the drivers of ecological processes and the vegetation-snow interactions at the treeline have been studied over a long period until now. In 1975, on a NE-exposed slope with average inclination of 38° and between 2000 and 2230 m a.s.l., 92 000 trees were systematically planted, counting for three species: European larch (*Larix decidua*), Swiss stone pine (*Pinus cembra*) and mountain pine (*Pinus mugo* subsp. *uncinata*). To observe the snow conditions, 400 snow laths were set and in one third of experimental area snow bridges were built. From the winter 1959/60 an intensive monitoring of snow and avalanches

began, snow depth was measured at the snow laths and the avalanches were systematically recorded on the daily basis (Bebi et al., 2009b).

3.2 Avalanche simulation with varying release and forest areas

In order to test different parameters, the avalanche at Teufi from 2008 was chosen for back calculation. The avalanche track is situated on the orographic left side of Dischmatal on the NE slope. The wet avalanche released from the slope ~40° due to rain-on-snow at night from 22nd to 23rd of April 2008 at 2080 m a.s.l. and flowed to the valley bottom at 1690 m a.s.l. (Figure 6).

Figure 6: Teufi avalanche from 2008 (Photo: Peter Bebi, 2008).

3.2.1 Release area

I systematically estimated the release area of the Teufi wet snow avalanche from 2008 through sensitivity analysis of fitting simulated runouts, by means of the zero maximum flow height. Various methods were used to determine the release area: upper

third of an avalanche (Bühler et al., 2013) changing the stauchwall according to slope inclination change or to the form of the observed avalanche, width=length (Yves Bühler, personal communication, July 2017), including or excluding forest within the release area in the upper part (Peter Bebi, personal communication, July 2017). I chose the optimal release area with respect to the runout direction and distance to match with the observed avalanche from 2008.

3.2.2 Avalanche parameters

For the simulation, scientific version of RAMMS was used. While simulating different scenarios of Teufi avalanche, the following parameters (Table 1) were fixed to test only the changing variables as different release areas and forest information.

Table 1: Parameters used for simulating the variants of Teufi avalanche in RAMMS.

Parameter	**Value**	**Unit**
release height	0.5	m
release ρ	350	kg/m^3
ξ	1000	m/s^2
μ	0.55	
cohesion	100	Pa
ρ	400	kg/m^3
T_0	-2	°C
w	0	mm/m^2
T_Σ	0	°C
w_Σ	5	%
erodibility	2	
epsilon	0	
generate	0.05	
decay (B)	1	1/s
act energy	2	kJ/m^3
μ wet	0.12	
dry-wet tr.	10	mm

3.2.3 Forest information

Using data from forest stand maps and orthophoto before the avalanche in 2008, I determined the forest parameters (forest type, crown coverage, roughness) to define the corresponding K-value using the look-up table for forest shape files (Figure 4). The necessary information (tree type = tree species, diameter at breast height, K-value) were assigned as attributes of polygons to serve as input file for RAMMS simulation. Forest polygons, within the first simulations for obtaining the optimal release area, were not including the area of green alder.

3.2.4 Green alder

After choosing optimal release area, I simulated the avalanche with forest including the area of green alder. RAMMS does not offer a special group for this particular tree species and the most similar tree type is birch (chosen K-value: 15). As green alder does not have the same characteristics as forest stand, in the next simulation I decided to include it as an area with specific frictional resistance to describe its influence on the avalanche. Green alder was included into separate shapefile, which was later used in RAMMS as an additional μξ-polygon. Friction value μ was fixed on 0.55 and I performed sensitivity analysis with ξ-values for friction (300, 500, 700 and 900 m/s^2). Runout distance, forest destruction and velocity were compared for different values of friction parameter ξ.

3.2.5 Destructive pressure

Destructive pressure of Teufi wet snow avalanche was calculated using sliding block model (SBM), which Feistl et al. (2015) determined as the most realistic with the highest bending stresses. For calculation of the SBM, we estimated the parameters as the avalanche volume length l_v and the angle ψ (depends on the location of the tree in the forest, terrain and avalanche dimensions).

The bending stress (σ) of the avalanche on the tree, using the sliding block model, is:

$$\sigma = \rho\ g\ l_v\ (l_v\ tan\psi + d)(sin\gamma - \mu\ cos\gamma)\frac{16\ h}{\pi d^2}{h_a}^2\ (cos\gamma)^2, \qquad (2)$$

where ρ avalanche density, g gravitational acceleration, h flow height, l_v volume length, ψ opening angle, d stem diameter, γ slope angle, μ friction angle, h_a impact height.

3.2.6 Forest scenarios

Three different scenarios were tested, increasing the forest density (crown coverage) to see, where the dense forest plays a more important role in stopping or hindering the avalanche flow. In the first possible scenario, I did not include forest to observe how the simulation output changes in the case of forest absence. The second scenario describes situation with dense forest right below the release area. Instead of the area of green alder, dense forest (K-value: 48) entered the simulation. The third scenario describes situation with dense forest in the middle part of avalanche track. Before the avalanche in 2008, forest in this area was specified as open (K-value: 28), which was in the third scenario substituted by dense forest (K-value: 48).

3.3 Comparison of field and remote sensing measuring methods

3.3.1 Field method

Before undertaking the fieldwork, I prepared an orthophoto plan using a grid of points 20x20 m. These points represent the centre of sample plots, which have 5 m in radius. In the field, two methods were used to locate the position: 1) In the area of Marteleskop (forest stand on the left side of the avalanche track looking upwards), the closest tree was chosen as the centre point of a plot. 2) Where no trees were measured in the past, GPS instrument was used to find the position of the plot centre.

Three different groups were chosen according to different forest type and density in terms of crown coverage (Figure 7 and Figure 8):

- Dense forest (DF) – crown cover ≥70 %,
- Open forest (OF) – crown cover <70 %,
- Green alder (GA) – lower forest stand composed of deciduous tree species, mainly green alder, rowan, willow and cherry tree.

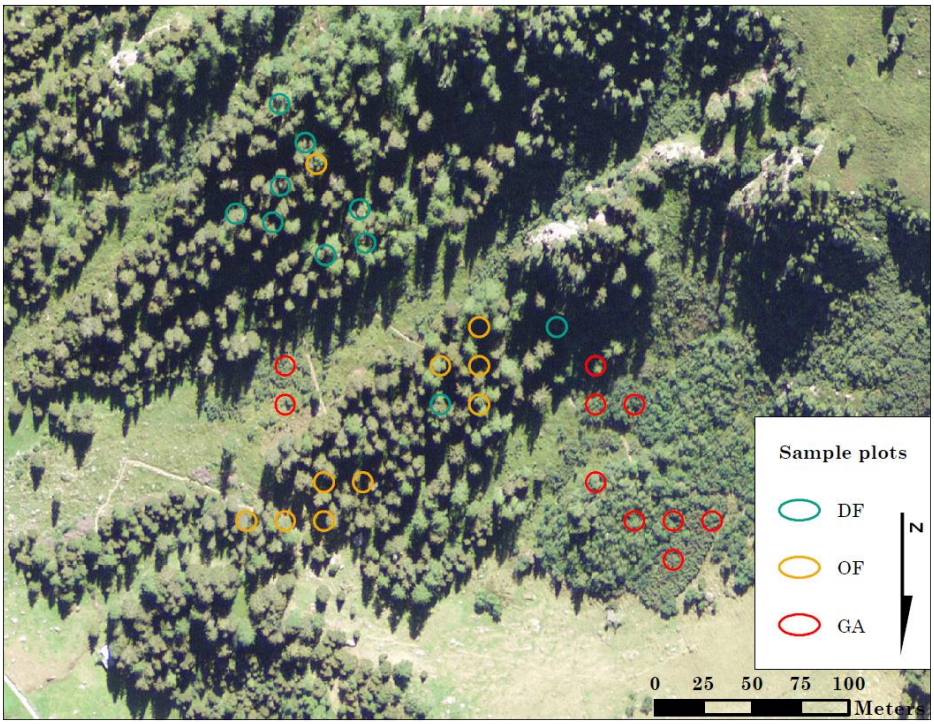

Figure 7: Sample plots in the forest of Teufi avalanche track. DF = Dense forest, OF = Open forest, GA = Green alder stand.

Every group consists of ten sample plots, where data on forest characteristics were collected, including: forest type, crown coverage, terrain roughness with its maximum relative height and main type of roughness; and tree parameters as tree species, DBH (diameter at breast height), tree height and forest layer. In the Marteleskop area, I took

all the tree parameters from already existing database from 2016. On these plots I collected information about forest type, crown coverage and terrain roughness.

Figure 8: Forest types: Dense forest (DF), Open forest (OF) and Green alder (GA).

3.3.2 Remote sensing methods

Vegetation height models (VHM and VHM_new)

The vegetation height model was calculated (Ginzler and Hobi, 2016) using digital aerial summer images in the years from 2007 to 2012. The Swiss Federal Office of Topography (swisstopo) collected the ADS80 stereo aerial images containing the data on vegetation heights, with spatial resolution of 0.25 m and 0.5 m for the mountain areas. Ginzler and Hobi (2016) used the aerial images to calculate a digital surface model with a resolution of 1 m. The difference between digital surface model and digital terrain model based on laser data produces the vegetation height model (VHM). Using this method, the resulting spatial resolution is useful for analysing entire forest stand, but not for single-tree-based analyses (Ginzler and Hobi, 2016). It is to be tested, how the resolution influences the accuracy of single parameter as maximal height, and the forest parameter (K-value), which enters the avalanche simulation.

The original VHM included in some areas less forest and the forest stands were too open. VHM_new has been corrected and a different threshold for forest definition was set, so it may happen that the forest is overestimated.

Digital surface model (DSM) and digital terrain model (DTM)

The digital surface model (DSM) and digital terrain model (DTM) were generated from airborne laser scanning (ALS). The data were collected in August 2015

using RiEGL LMS-Q 780. The resulting DSM and DTM have both high resolution of 0.5 m.

3.3.3 Maximal tree height

After collecting the data, the maximal tree height within the 30 sample plots (Figure 7) was compared with the maximal tree height from the digital data (VHM, DSM-DTM and corrected VHM). The measured maximal tree height was also compared to the heights measured by remote sensing methods at the Stillberg area, using already existing database of tree information including the tree heights. To find statistically significant difference between the methods, following tests were used: constancy of variance, Fligner-Killeen test of homogeneity of variances, one-way ANOVA and post-hoc Tukey's test (Crawley, 2007).

3.3.4 Forest information

To be able to assign the K-values, first, the forest polygons had to be mapped and the forest characteristics set. As described in Figure 10 different approaches were used to define the forest polygons and to assign the corresponding K-value for the field method and remote sensing method. The first step was to recognize the forest. In the field method, the forest was visually classified from orthophoto, and in the remote sensing method the height classification was used.

3.3.5 Height classification of remote sensing data

To recognize trees from shrubs and herbal vegetation from remote sensing data I used height classification (Table 2). As stated by the international forest definition, forest is land with tree crown coverage minimum 10 percent, area 0.5 ha and tree height minimum 5 meters (FAO, 1998; FRA 2000; UNFCCC, 2001). This 5 meters threshold was used to differentiate forest from other lower vegetation. To include green alder in the classification, another threshold of 1 m was taken to exclude the herbal vegetation, so the resulting interval for green alder is 1-5 m. Green alder grows with a height between 0.5-5 m [1]. This corresponds to field observed heights that were maximum 4 m for a green alder. The other deciduous species as rowan (*Sorbus aucuparia*), birch (*Betula* sp.), willow (*Salix* sp.), cherry tree (*Prunus avium*), are classified in the interval

between 5 and 10 m. For the forest stand classification, trees higher than 10 m with adjacent 5-10 m trees were taken. For the green alder classification, I used the intervals 1-10 m (green alder plus other deciduous trees).

Table 2: Vegetation height classification for remote sensing data.

Height [m]	Vegetation type
0	no vegetation
0-1	herbal vegetation
1-5	green alder
5-10	other deciduous and younger trees
>10	high forest

3.3.6 Terrain roughness

The terrain roughness was obtained (processed by Yves Bühler, October 2017) from DTM using the vector ruggedness measure developed by Sappington et al. (2007). This method compares vectors of slope and aspect of the neighbouring pixels around the central pixel (Figure 9). The size of used neighbouring window was 5x5 pixels and DTM resolution of 0.5 m. The resulting roughness is a value between 0 (flat) and 1 (extremely rough).

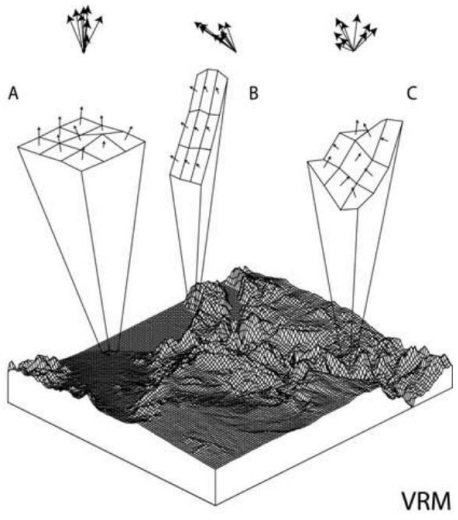

Figure 9: Vector dispersion method according to Sappington et al. (2007). The variability in vectors defines the surface roughness.

Terrain roughness was classified into three classes (smooth, knobby, rough) with threshold values 0.01 and 0.02 considering the values found in literature (Sappington et al., 2007; Sovilla et al., 2012; Bühler et al., 2013; Veitinger and Sovilla, 2016, Veitinger et al., 2016). The median roughness value for every of the 30 sample plots (Figure 7) was calculated and assigned to a roughness class (Figure 29). The roughness derived from DTM was compared to the roughness observed in the field.

3.3.7 K-values classification

The second step after the forest recognition is to choose the characteristics of forest area to obtain the corresponding K-value according to the look-up table in Figure 4. Forest type is classified by observation in the field or using the forest stand maps. It is also possible to recognize several tree species visually using the orthophoto. Crown coverage is determined analysing the orthophoto or according to the height classification, where big differences between heights occur (tree vs. ground). Next step is determining forest polygons using both forest type and crown coverage to obtain homogeneous areas. Afterwards terrain roughness is assigned from field observation or derived from DTM, where the median terrain roughness is calculated for each polygon (using Python formula Zonal Statistics). This median is assigned to the corresponding roughness class (smooth, knobby or rough). After having all this information, K-value can be assigned (Figure 10).

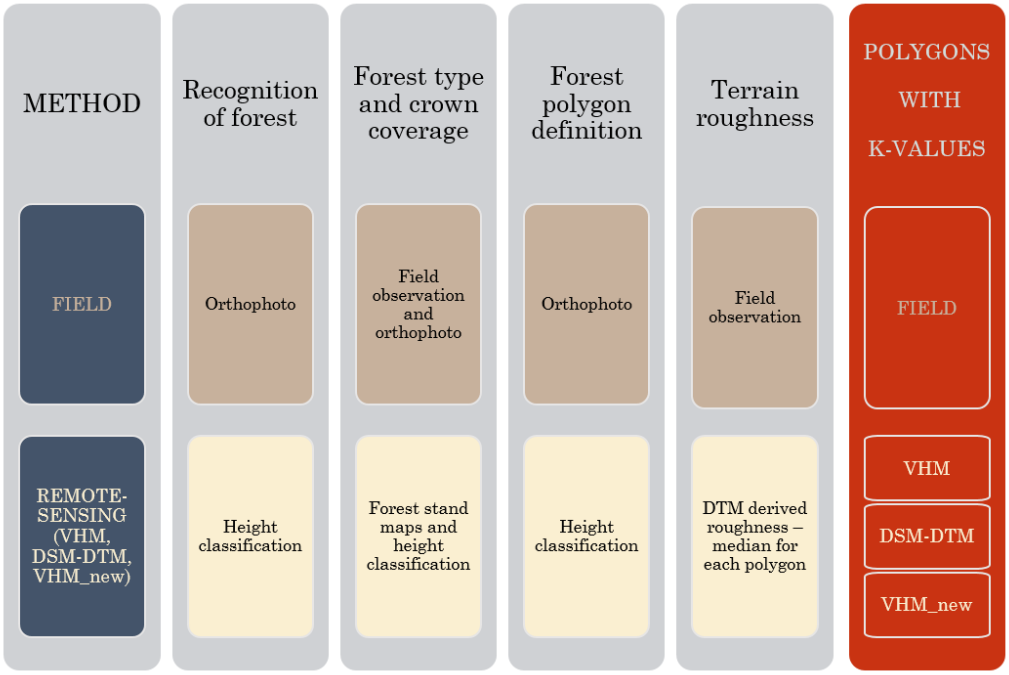

Figure 10: Process of K-value classification for the field and remote sensing methods.

3.3.8 Diameter at breast height (DBH)

To complete the forest input shapefile, it is necessary to add the DBH into the attribute table for each polygon. It is possible to collect this parameter in the field, use forest stand maps or calculate it from the heights obtained by remote sensing. In the remote sensing methods, all heights under 5 m have to be removed and calculate the median height for each forest polygon. From the median height, the DBH in every polygon is calculated, using a simple formula from RAMMS for height estimation, where

$$DBH = H^{1.25} \rightarrow H = DBH^{0.8}. \quad (3)$$

The method of calculating the DBH using RAMMS formula is tested comparing the calculated DBH with the measured DBH from 2015 at Stillberg area. Three different tree species are present with different number of individuals: 536 individuals of Swiss stone pine (*Pinus cembra*), 980 individuals of mountain pine (*Pinus mugo* subsp. *uncinata*) and 2649 individuals of European larch (*Larix decidua*).

3.3.9 Comparison of the K-values

The differences in K-values between the Field method and the remote sensing methods were calculated (using the Raster calculator). The differences were displayed using red colours for the negative difference (Field method having higher values) and blue colour for the positive difference (Field method having lower values). The shading shows the magnitude of the difference with darker colours for bigger absolute difference (Figure 32).

3.3.10 Comparison of the simulation outputs

All the simulation outputs using the four different methods were compared visually on orthophoto, similarly to Teich et al. (2014), and assessed according to the differences in the maximum values over time for velocity, pressure and flow height. To compare the runout distances, the maximum flow height was used and the threshold was set to zero meters, which would correspond to the observed impacted area of an avalanche in the field.

3.4 Tree-snow interaction in the initial stages of forest succession

For the analysis of snow-tree interaction, only a part of Stillberg area was used, where no avalanche bridges are present (Figure 11). This area was divided around the snow laths into 144 plots. Correlation analysis was carried out between the maximal snow height and the number of trees and the tree heights within these plots. To check the influence of the elevation, test of correlation using the snow lath elevation and the maximal snow height was performed.

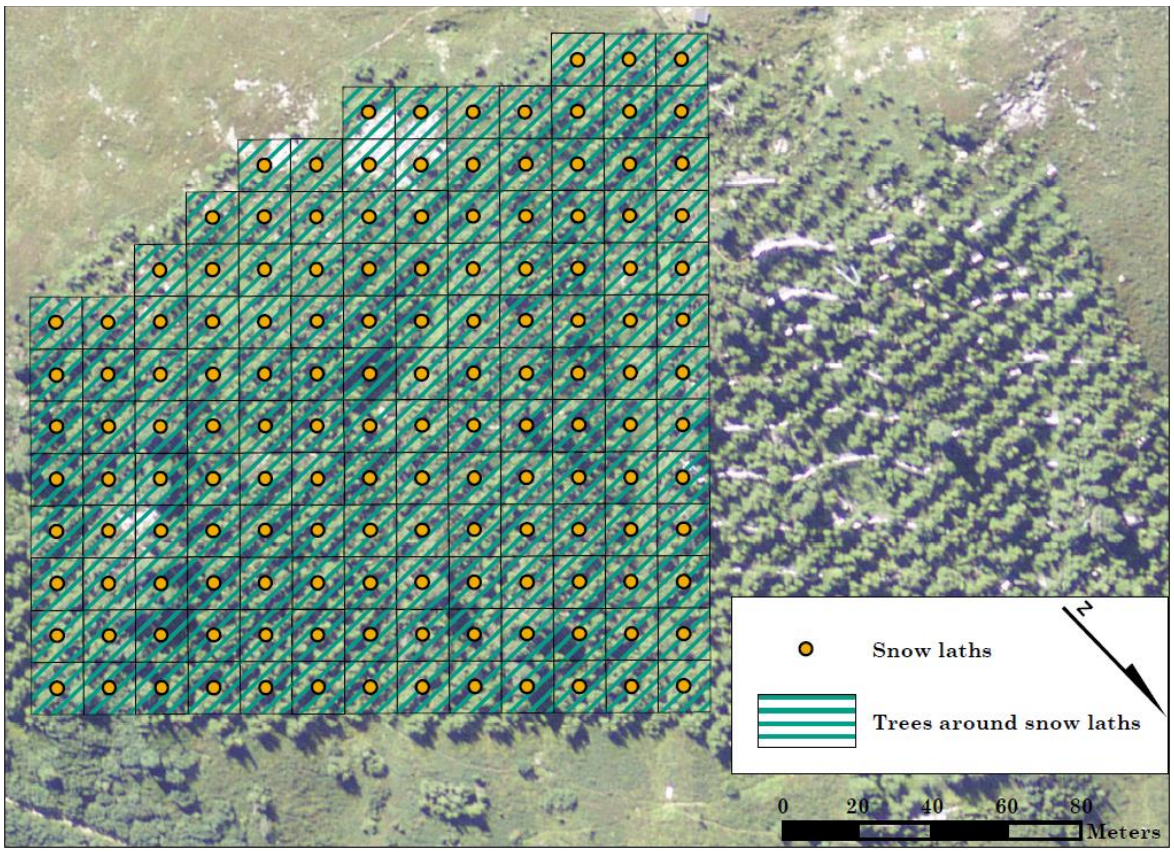

Figure 11: Stillberg afforestation with snow laths, where the snow was measured and areas around these laths with trees.

3.4.1 Avalanches at Stillberg

Observed avalanches from 1976 to 2003 were mapped by hand on 1:500 topographic maps and then digitized as shapefiles. The avalanches from 2003 onwards were not systematically observed, but their occurrence was discussed with local people and SLF employees (Christian Simeon and Peter Bebi), and derived from documented photographs (Appendix A: Figure 41 and Figure 42). For the descriptive statistics, I

only used the avalanches that released on the side of Stillberg area, where no avalanche bridges are present.

The total number of avalanches from whole Stillberg area in the available time span from 1960 to 1995 was taken from the database of avalanche mapping in Davos. This unique database consists of recorded avalanches since the winter of 1949/50. SLF staff in cooperation with rescue services, and stuff of the mountain railways/cableways have recorded and mapped the avalanche outlines on the area of 150 km^2, including ski touring and freeriding areas as well as areas relevant to transport and settlement. They have recorded all slab avalanches with a minimum size of 50 m in one direction and loose-snow avalanches with minimum length of 100 m. Two main sources of recording errors are the impaired visibility during snowfall and windy conditions, and the absence of avalanches covered with fresh snow, which were not observed. During an increase of avalanche activity, photographs are used to record avalanches, which are mapped afterwards [2]. However, it is not easy to define the avalanches from the terrain to the maps and many errors occur during this process. The biggest challenge is to transform the 3D information to 2D maps especially in wintertime, when the snow covers the terrain features, which are not fully visible (Bühler et al., 2013).

4 Results

4.1 Avalanche simulation with varying release and forest areas

4.1.1 Release area

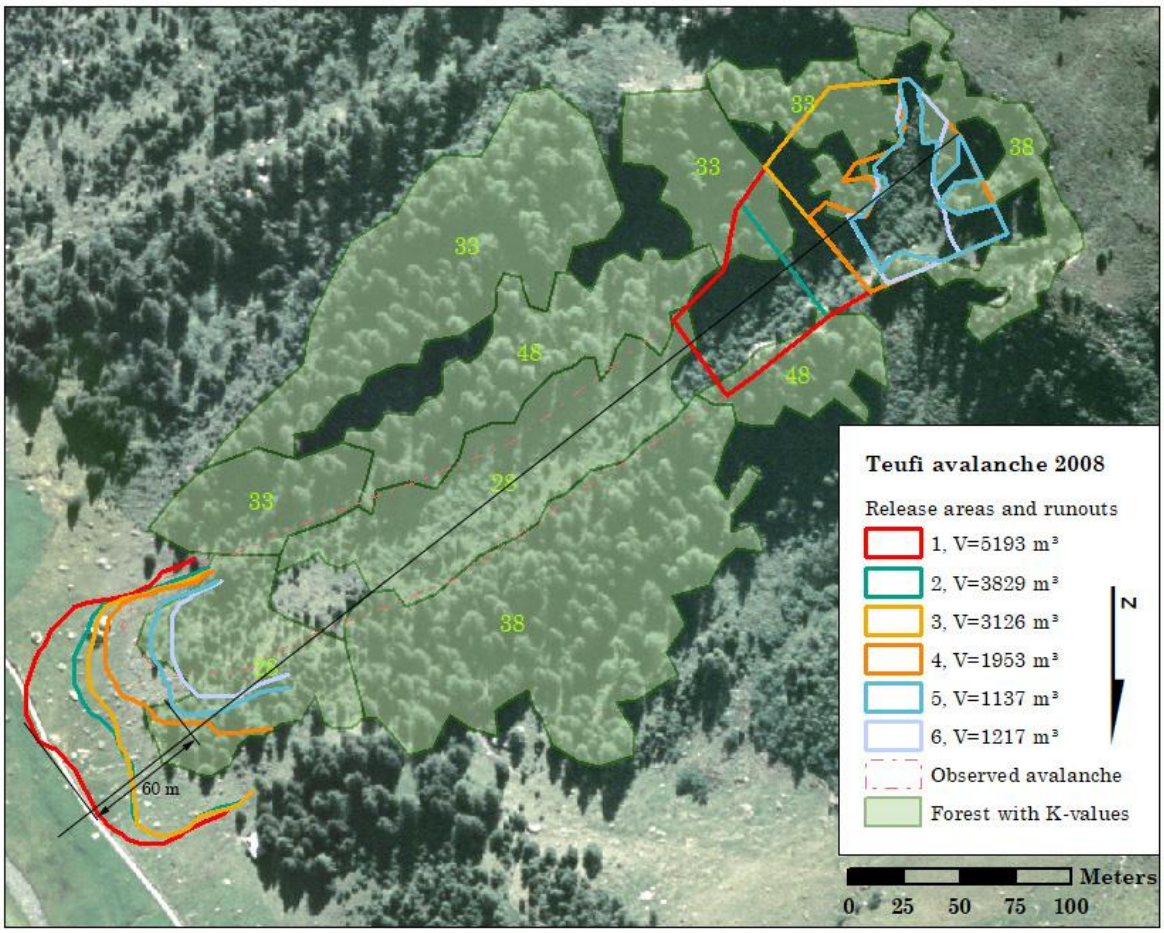

Figure 12: Testing different release areas. Increasing the size of release area, the corresponding runout becomes longer. Forest was represented by shapefile with different K-value for every homogeneous forest stand.

Choosing the release area as one third of the observed avalanche produced the longest runout distance (number 1 in Figure 12). The runout distance is decreasing with smaller release area. The release area, without including the forest in the upper part (number 5 in Figure 12), produced the most similar avalanche runout to the observed one from the year 2008. This runout is 60 m shorter in comparison to the longest runout (number 1 in Figure 12).

4.1.2 Green alder

After choosing the optimal release area with respect to all set parameters, the focus was brought on green alder that was tested as forest stand (K-value: 15). In this simulation, forest destruction was observed also within the green alder stand, where in reality no destruction happened. By including the green alder as forest, the runout distance has decreased and the avalanche stops in the lower open forest (Figure 13).

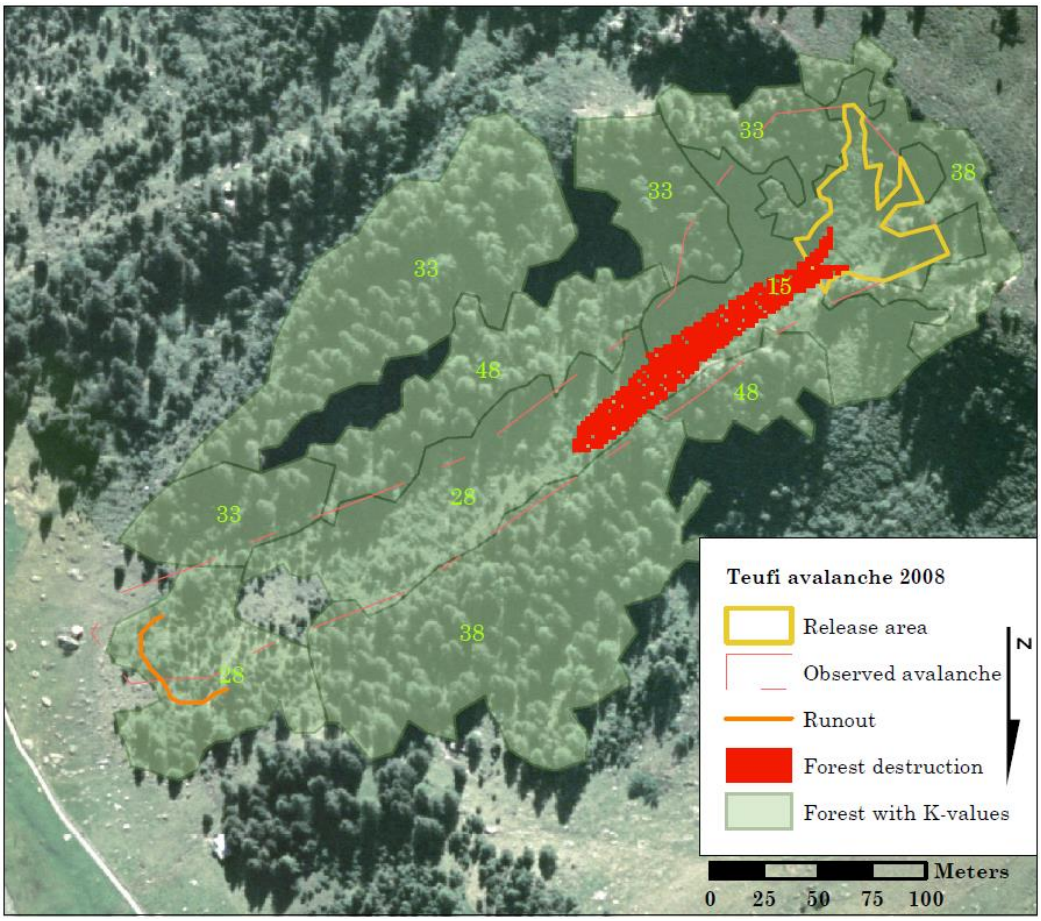

Figure 13: Green alder area tested as a forest polygon with K-value 15 results in large forest destruction and shorter runout distance than the runout of the observed avalanche.

The green alder was afterwards tested as an additional friction parameter, using sensitivity analysis for different ξ-values, resulting in more realistic outputs than by handling the green alder as a forest stand. With increasing roughness (decreasing ξ-value), the runout distance and velocity decreases. The runout distance by ξ=300 m/s² is underestimated by about 25 m. For ξ=500, 700 and 900 m/s² runout distance is realistic comparing to the runout distance of the observed avalanche. Maximum velocity of ξ=300 m/s² is 14.75 m/s and the highest maximum velocity occurs by ξ=900 m/s² and is 22.20 m/s, respectively (Table 3). For ξ=300 m/s² and ξ=500 m/s²,

forest destruction does not occur compared to ξ=700 m/s² and ξ=900 m/s², where with higher ξ value, forest destruction increases (Figure 14). The optimal simulation output considering the runout distance and the forest destruction in the higher part of the forest is with the ξ=700 m/s²; however the forest destruction in the lower part of the avalanche track is underestimated.

Table 3: Sensitivity analysis of ξ values for green alder area and corresponding resulting velocities.

ξ (m/s²)	max velocity (m/s)
300	14.8
500	18.7
700	20.6
900	22.2

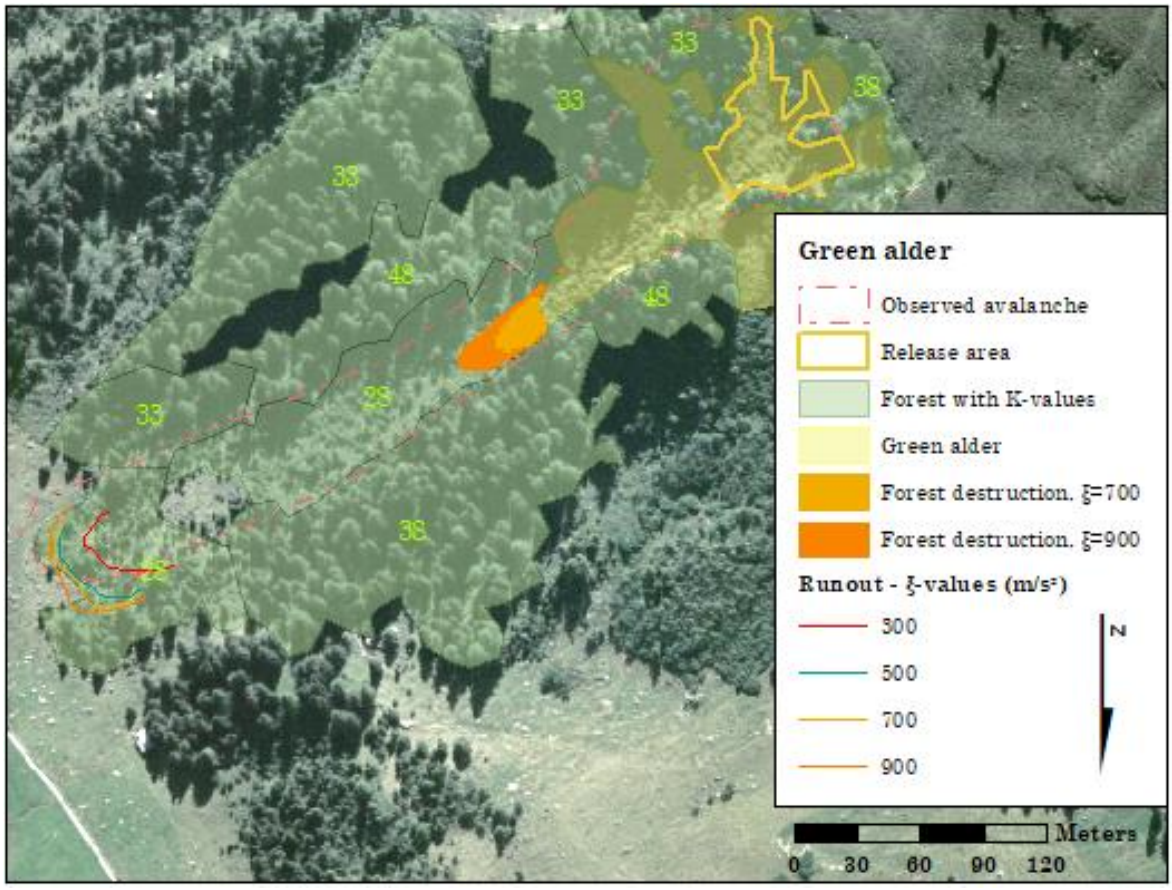

Figure 14: Testing the green alder area as an additional friction parameter using sensitivity analysis for different ξ-values (ξ= 300, 500, 700 and 900 m/s²), results in longer runout distances with increasing ξ-value and also increasing forest destruction, which occurs by ξ= 700 and 900 m/s².

4.1.3 Destructive pressure

Using the sliding block model to calculate destructive pressure, it was revealed that the trees in the lower part of the avalanche track are destroyed which corresponds with the observation (Figure 6). The value of calculated bending stress (σ) of the lower part of Teufi avalanche is 39.6 MPa.

4.1.4 Forest scenarios

Scenario without forest (scenario #1) has overestimated runout, stopping only due to the flat terrain in the area of the hiking path (Figure 16). The runout distance is 60 m longer than the runout of the avalanche from 2008. Its maximal velocity reaches 23.36 m/s in comparison to scenario with dense forest in the release area and scenario with dense forest in the avalanche track with maximum velocities of 20.7 m/s and 21.59 m/s, respectively.

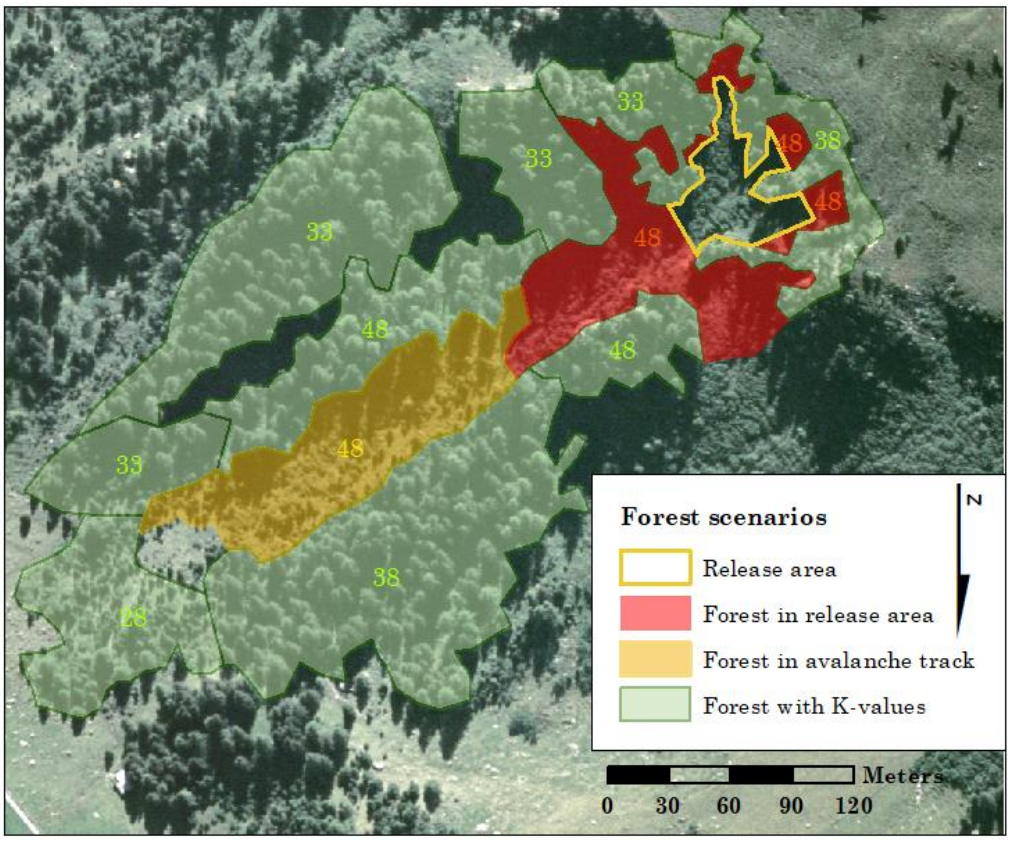

Figure 15: Forest scenarios with dense forest right below the release area (scenario #2) and within the avalanche track (scenario #3).

Both scenarios with dense forest have shorter runout distance than the observed avalanche. In the case of the scenario with forest in the avalanche track (scenario #3,

Figure 15), runout distance shortens by 80 m and the other scenario with dense forest just below the release area (scenario #2, Figure 15) shortens by 50 m with respect to the runout distance of an observed avalanche (Figure 16). Interestingly by higher velocity in the avalanche track, no forest destruction occurs, due to higher DBH values in the dense forest stand. In the scenario with dense forest just below the release area, forest within the avalanche track gets destroyed.

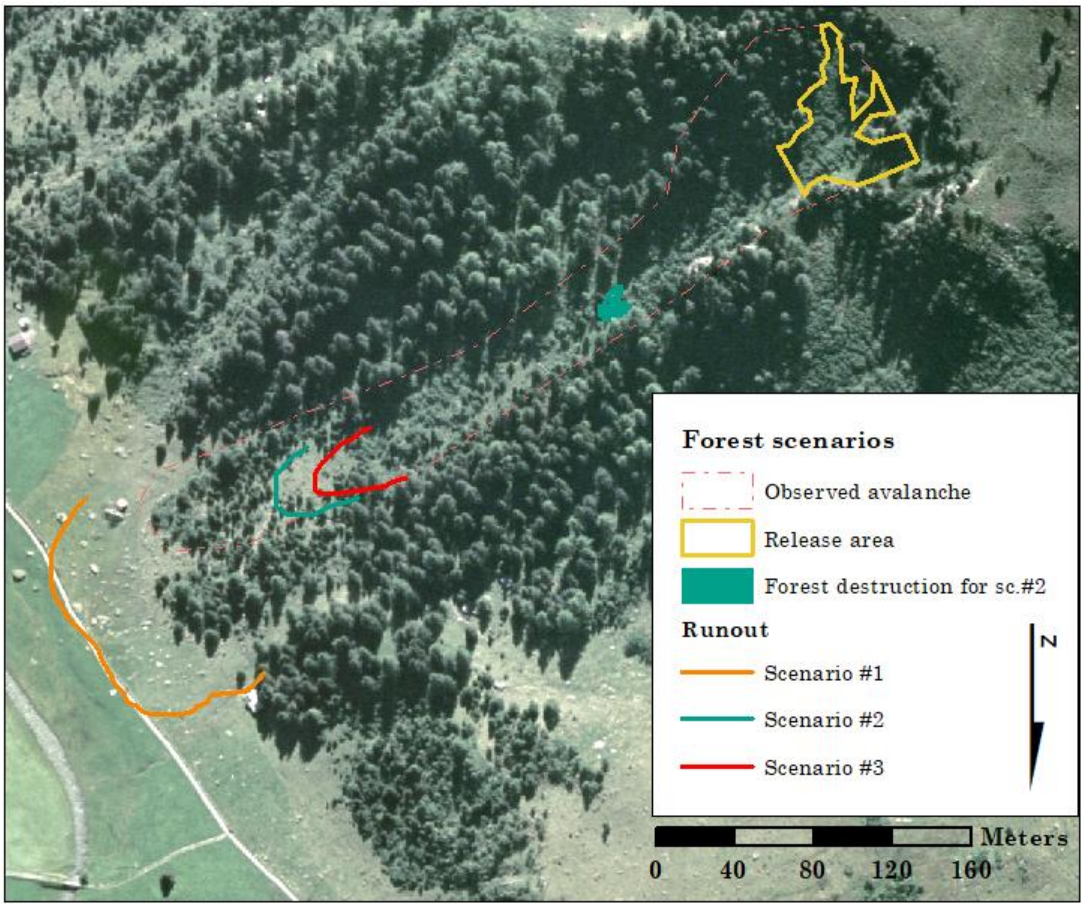

Figure 16: Forest scenarios with dense forest right below the release area and within the avalanche track. Resulting runout distances by three different forest scenario (dense forest in the release area or within the avalanche track and no forest scenario. No forest scenario has the longest runout distance. Dense forest in the release area results in the shortest avalanche runout.

In the scenario #2 (with forest just below the release area), some snow detrained in the upper part, and due to high velocity in that area, the avalanche disturbed part of the forest in the middle (Figure 16) and then deposited behind the trees in the lower part (Figure 17). In the scenario #3 most of the snow detrained right after entering the forest and in the lower part only small amount of snow detrained. More snow detrained in the scenario #3 (877 m^3) in comparison to the scenario #2 (839 m^3).

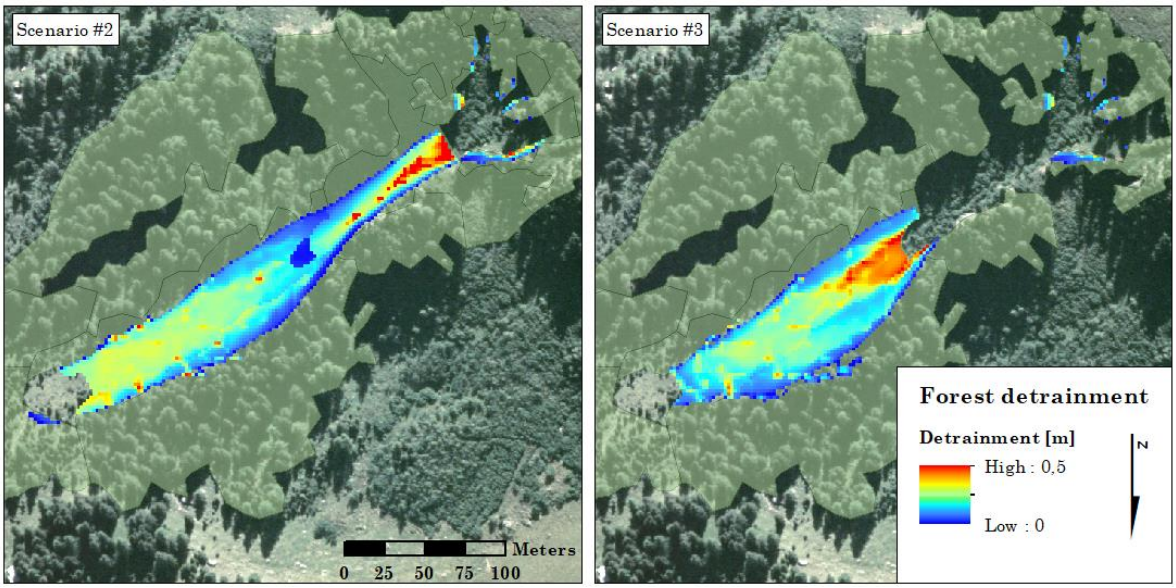

Figure 17: Forest detrainment. Different amounts of snow detrained in the two scenarios with dense forest right below the release area (scenario #2) and with the dense forest in the avalanche track (scenario #3). In the scenario #2 more snow detrained in the lower part of the forest in comparison to the scenario #3.

4.2 Comparison of field and remote sensing measuring methods

4.2.1 Determining forest polygons

According to the forest type and the crown coverage, forest (black line in Figure 18) and green alder (light grey line in Figure 18) polygons were manually created. The biggest differences in forest polygons can be seen in the VHM_new, where only few big polygons were created, because the model smoothened the heights within the forest and excluded the forest gaps (VHM_new in Figure 18). The VHM resulted in similar forest polygons as from the orthophoto, however the green alder stands within the avalanche track were not detected by this model. The most precise output is delivered from the difference between DSM and DTM (DSM-DTM in Figure 18), which both have high resolution of 0.5 m. The shadow on orthophoto does not allow a proper forest classification as well as on the not corrected VHM, where the most problematic parts are within the avalanche track resulting in no green alder polygons.

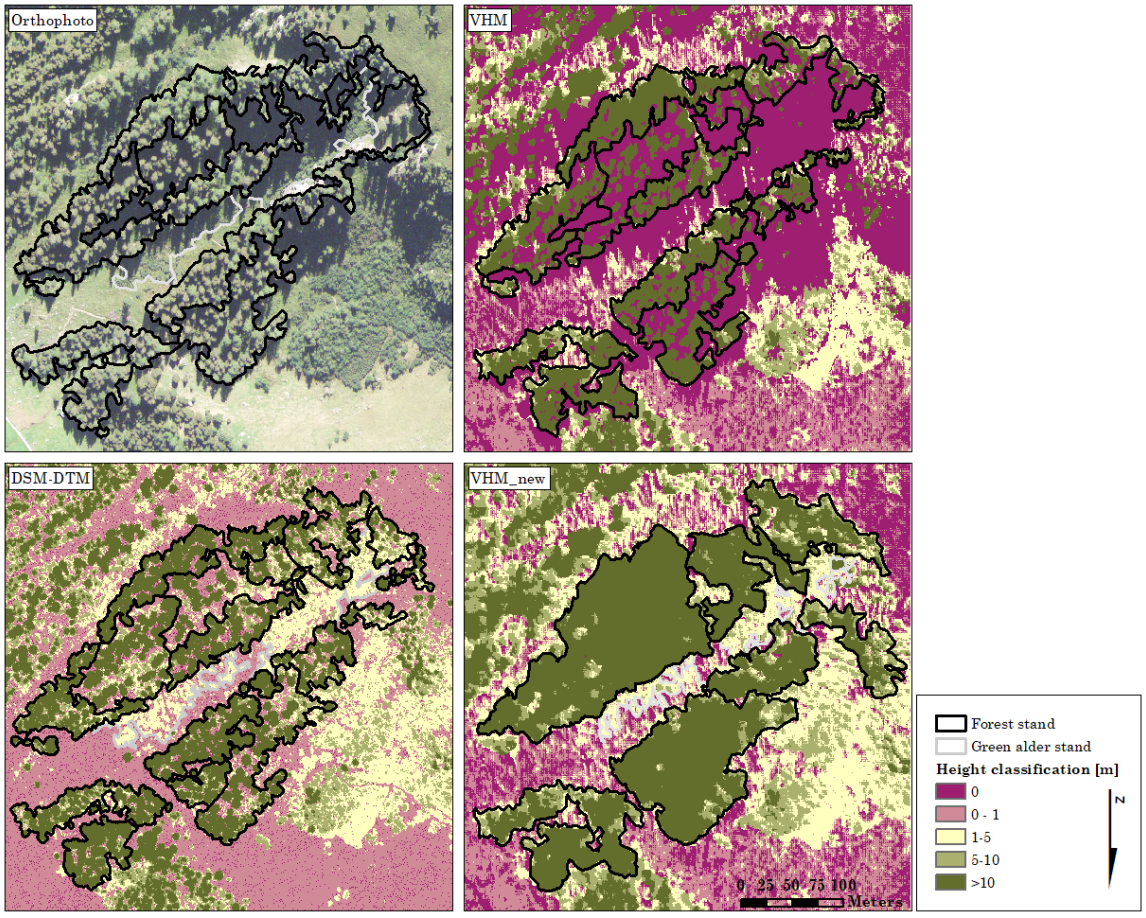

Figure 18: Forest and green alder polygons for field and remote sensing methods. Polygons are defined visually from orthophoto for the field method and according to the height classification for the remote sensing methods.

4.2.2 Maximal tree height - Teufi

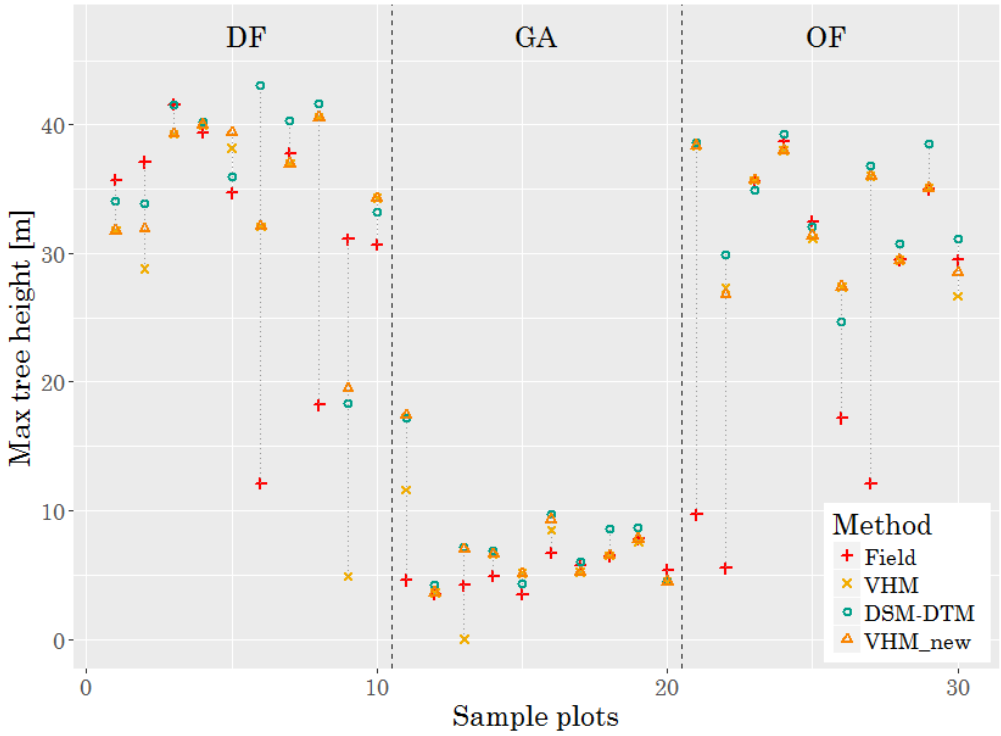

Figure 19: Sample plots and corresponding maximal height per plot measured using four different methods (Field, VHM, DSM-DTM, and VHM_new). The lowest variance is in the Green alder group (GA) and in the Dense forest (DF) and Open forest (OF) higher variance occurs.

Differences between field-measured tree heights as measured by different remote sensing data varied according to vegetation type (Figure 19). The smallest differences between the four methods were found for the vegetation type Green alder (GA). Comparatively large differences occur between different measuring methods for some samples within the groups of Dense forest (DF) and Open forest (OF). The Field method generally shows the smallest values for the maximal height per plots and the DSM-DTM overestimates the maximal heights compared to the Field method.

Testing constancy of variance (Crawley, 2007), the results of each method do not show any difference between the variances (variances s^2: 204.67 m^2 in the Field method, 207.88 m^2 for VHM method, and for methods DSM-DTM and VHM_new these values were 199.65 and 183.60 m^2, respectively). Using the Fligner-Killeen test of homogeneity of variances (Crawley, 2007) the results showed no evidence of any significant difference in variance across the four methods (p-value = 0.9371). Each of the two tests shows no evidence of any significant difference in variance across the four measuring methods, so it is appropriate to continue with one-way analysis of variance.

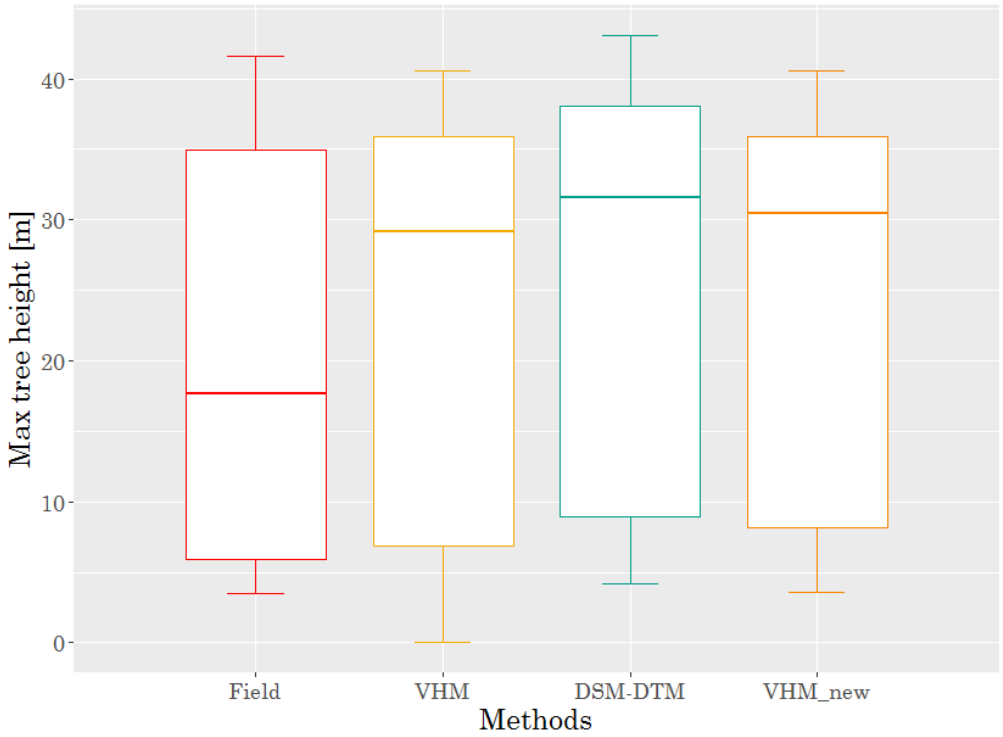

Figure 20: Distribution of measured maximal heights. Most of the samples have the similar distribution using different measuring methods; however, the median of the Field method is much lower (17.7 m) compared to the remote sensing methods having higher median, with the highest one for the DSM-DTM method (31.6 m).

There is considerable variation in samples within all measuring methods, although the boxes are overlapping with no big difference. The lowest value was measured with VHM method and the biggest value for maximum height goes over 40 m in all four methods. Median height is much lower using the Field method (17.7 m) compared to the other methods. The remote sensing methods have similar medians around 30 m and the highest median is using the DSM-DTM method (31.6 m). (Figure 20).

Figure 21: Distribution of measured maximal heights. The total sum of squares (SSY = 23558.14) as the sum of squares of the distance between each data point to overall mean (dashed grey line) and the error sum of squares (SSE = 23078.06) is the sum of the squares of the distance between each data point to its particular method mean (coloured dotted lines).

The total sum of squares (SSY = 23558.1 m²) is the sum of the squares of the distance between each data point to overall mean (dashed grey line in Figure 21). The error sum of squares (SSE = 23078.1 m², corresponding to the variance s^2 = 198.9 m²) is the sum of the squares of the distance between each data point to its particular method mean (coloured dotted lines in Figure 21). The standard deviations are 14.3 m, 14.4 m, 13.5 and 14.1 m in Field, VHM, DSM-DTM and VHM_new method, respectively. In this case, the total distance to the points in SSE is shorter than in SSY. This difference is a measure of significance of the difference between the mean heights within the methods. This shows that there is no significant difference between the four different methods (Figure 21). All the assumptions for the model are fulfilled (Figure 43 in Appendix B).

Table 4: ANOVA table: Testing the null hypothesis that there is a difference between the mean maximal heights using different methods.

Source	**Sum of squares**	**Degrees of freedom**	**Mean square**	***F* ratio**	***p* value**
Measuring method	480.0	3	160	0.804	0.494
Error	23078.1	116	s^2 = 198.9		
Total	23558.1	119			

The means of the Field method and the remote sensing methods do not significantly differ on the 5% level (accepting the null hypothesis that the method means are all the same, because F ratio = 0.804 is smaller than the critical value of F value = 2.683). In addition, testing the cumulative probabilities of the F distribution (p-value results in 0.494), the probability the null hypothesis is true, is almost 50% and that indicates no significant difference between the methods (Table 4).

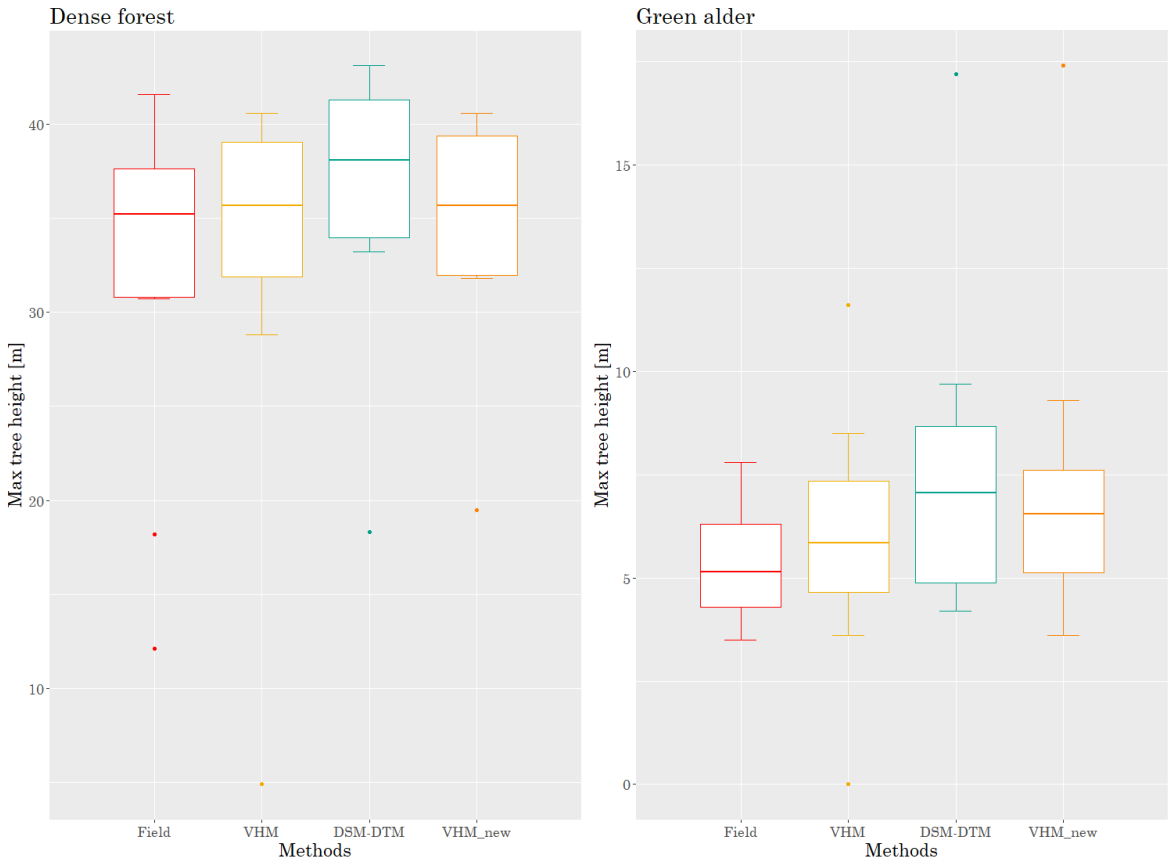

Figure 22: Data distribution using different measuring methods in two groups of forest type: Dense forest (on the left) and Green alder (on the right). In both groups, the highest median is using the DSM-DTM method and the lowest median is when using the Field method.

Testing the same methods using the samples only within one group of forest type (Dense forest, Green alder and Open forest), the methods within the groups of Dense forest and Green alder were not found significant different, with p-values 0.668 (Dense forest) and 0.301 (Green alder). In both groups, the lowest median is using the Field method and the highest by DSM-DTM method (Figure 22).

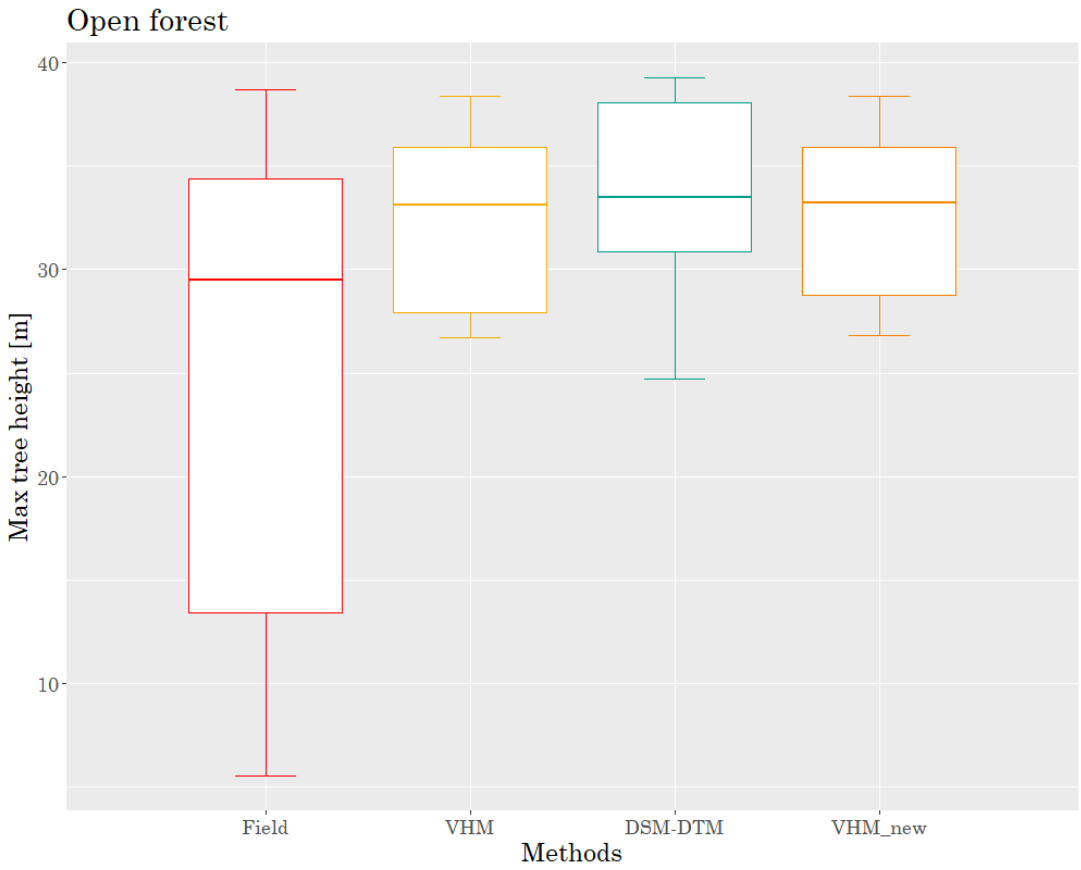

Figure 23: Data distribution using different measuring methods in the forest type: Open forest. The highest median is using the DSM-DTM method and the lowest median is when using the Field method. The Field method has a large variation between the samples.

In the group of Open forest, the lowest median is when using the Field method and the highest by DSM-DTM method. High variation in samples occurs within the Field method compared to the remote sensing methods (Figure 23). The difference between the method means is significant at 5% with p-value = 0.028 (Table 5).

Table 5: ANOVA table: Testing the null hypothesis that there is a difference between the mean maximal heights using different methods in the sample group Open forest.

Source	**Sum of squares**	**Degrees of freedom**	**Mean square**	***F* ratio**	***p* value**
Measuring method	540.6	3	180.22	3.398	0.028
Error	1909.2	36	$s^2 = 53.03$		
Total	2449.8	39			

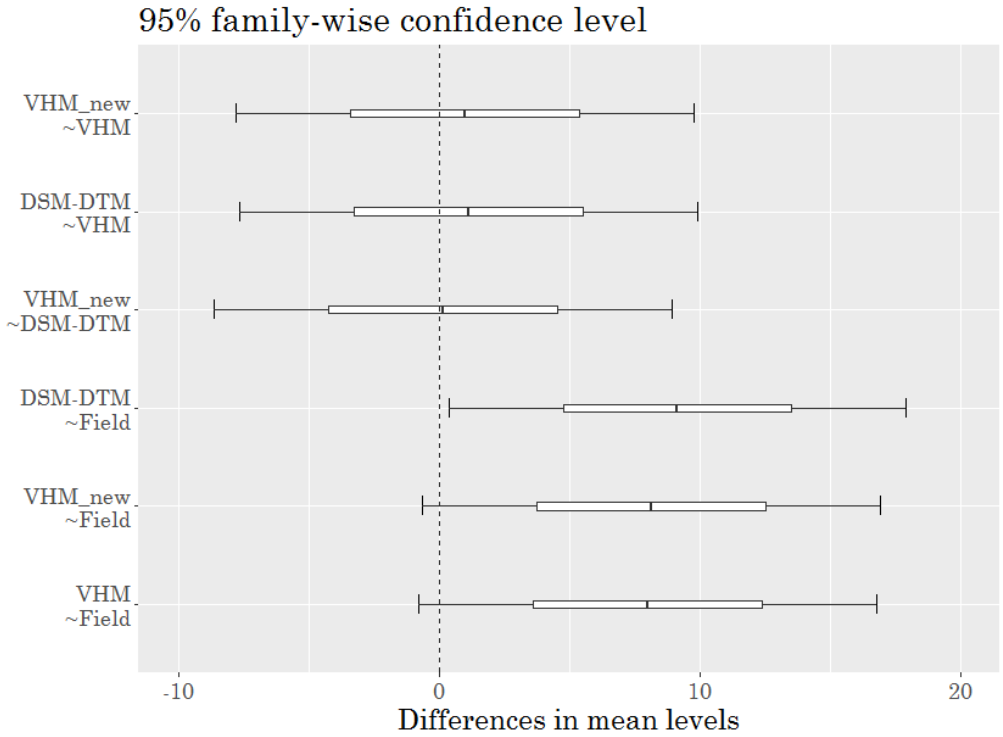

Figure 24: Post-hoc TukeyHSD: Significantly different means for Open forest are Field and DSM-DTM methods. The Field form the VHM method and the VHM_new method vary almost significantly in the 95% confidence level.

Within the Open forest group, the Field method differs from the DSM-DTM method (Post-hoc analysis with Tukey's test with p-value 0.0384; Figure 24). Whereas comparing Field method to the others, there is no significant difference (with VHM p-value 0.0845 and VHM_new p-value 0.0765).

4.2.3 Maximal tree height – Stillberg

The height classification differ within the three remote sensing methods (Figure 25). VHM_new has smoothened the forest gaps, so the expected resulting maximal height has higher values than using the VHM method. Looking at the DSM-DTM map, forest gaps have mainly the values between 0-1 m in comparison to the other two remote sensing methods, where the prevailing value within the forest gaps is 0. Also in the lower part, DSM-DTM method shows higher values for the high individual trees (values above 10 m).

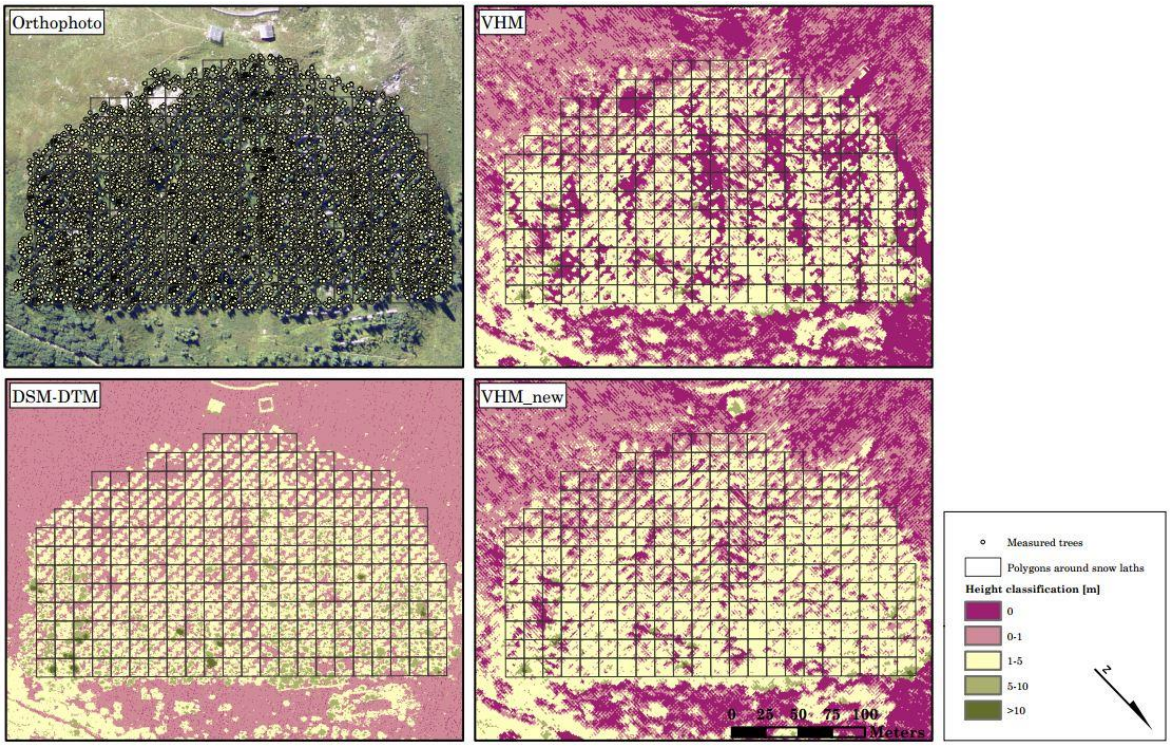

Figure 25: Comparison of field and remote sensing methods. Within the polygons around snow laths, measured heights are compared to the heights derived from the three remote sensing methods (VHM, DSM-DTM and VHM_new).

From the Figure 26 we can observe that the elevation correlates with the tree height for the field and remote sensing methods (Pearson's negative correlation is significant for all four methods with p-value <0.001, with correlation value -0.5).

According the DSM-DTM method, all maximal heights are overestimated, whereas VHM and VHM_new are predicted well comparing them to the Field method (Figure 26).

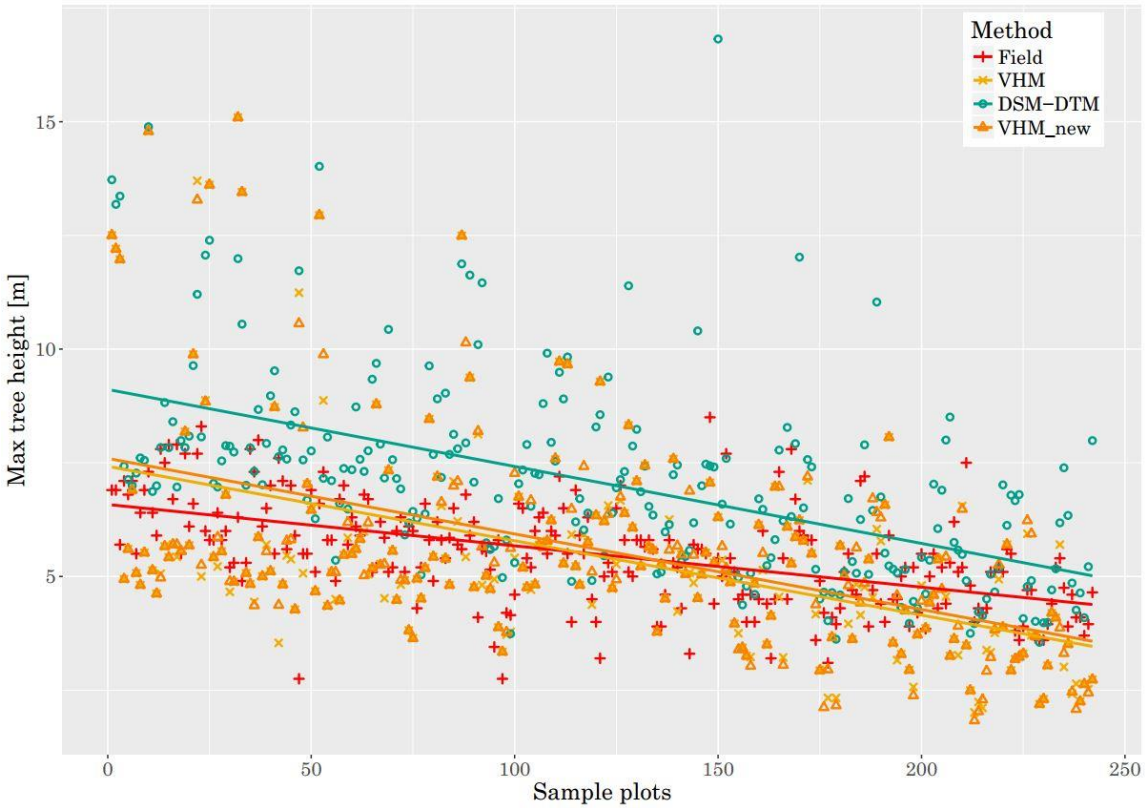

Figure 26: Sample plots and corresponding maximal height per plot was measured using four different methods (Field, VHM, DSM-DTM, and VHM_new). The method DSM-DTM overestimates the maximal heights.

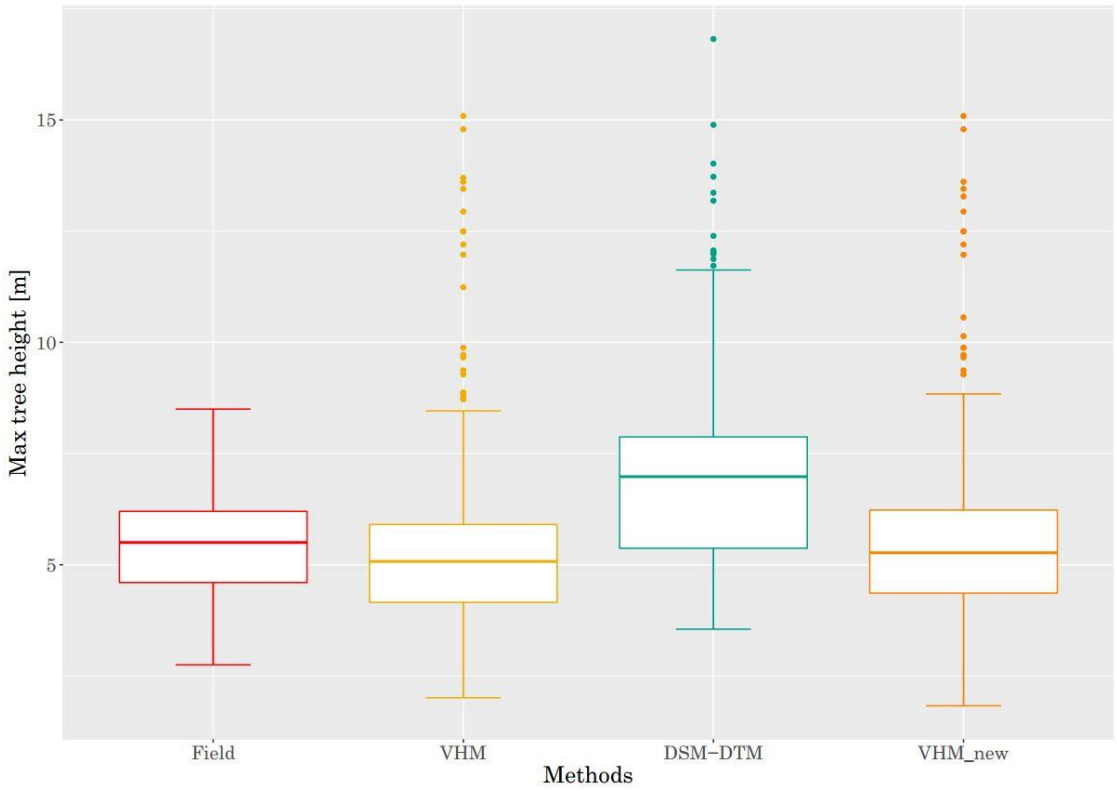

Figure 27: Distribution of maximal tree height using different measuring methods at the Stillberg area. The highest median is when using the DSM-DTM method, which has also larger variation between the samples than the other methods.

The field and remote-sensing methods measuring the maximal height are significantly different (ANOVA analysis with *p*-value <0.001; Table 6). Higher variation in samples occurs within the DSM-DTM method compared to the other methods (Figure 27). The lowest median is when using the VHM method and the highest by DSM-DTM method.

Table 6: ANOVA table: Testing the null hypothesis that there is a difference between the mean maximal heights using different methods.

Source	Sum of squares	Degrees of freedom	Mean square	F ratio	p value
Measuring method	443.9	3	147.9	35.94	<0.001
Error	3967.0	964	4.12		
Total	4410.9	967			

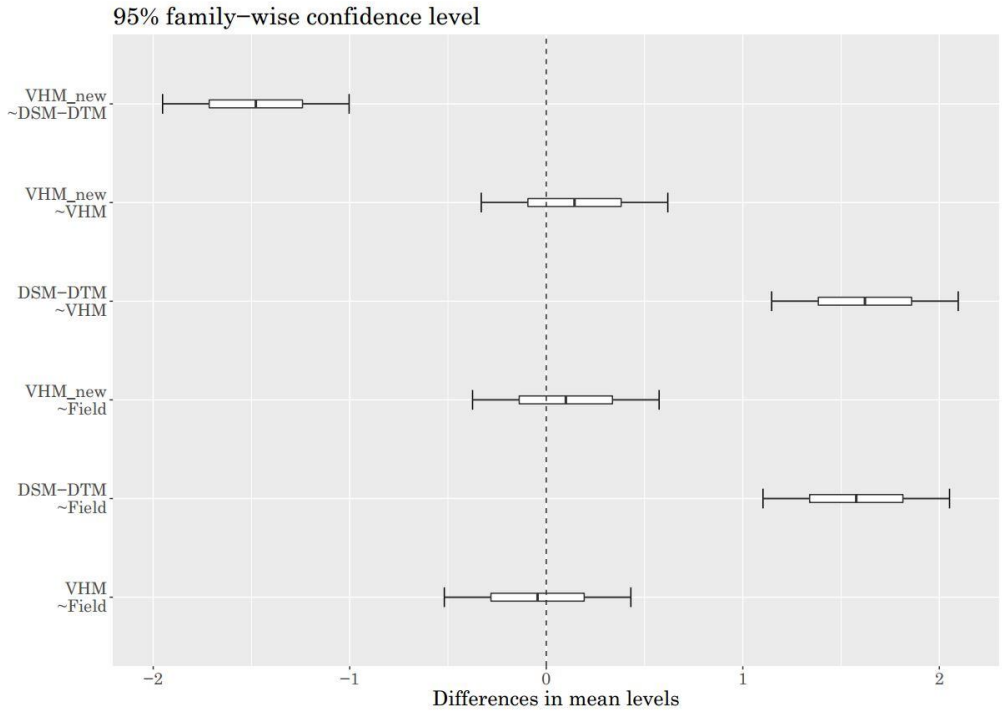

Figure 28: Post-hoc TukeyHSD: Different means has the DSM-DTM method comparing it to the others, with the p-value = 0 in all three cases.

The DSM-DTM method differs from all of the other methods (Post-hoc analysis with Tukey's test, *p*-value <0.001). Other methods do not vary among each other (Figure 28).

4.2.4 Terrain roughness

Figure 29 shows terrain roughness classified into three classes (smooth, knobby, rough), using thresholds 0.01 and 0.02 for the calculated roughness from a high resolution DTM. For every of the 30 plots median roughness value was calculated and then assigned to roughness class.

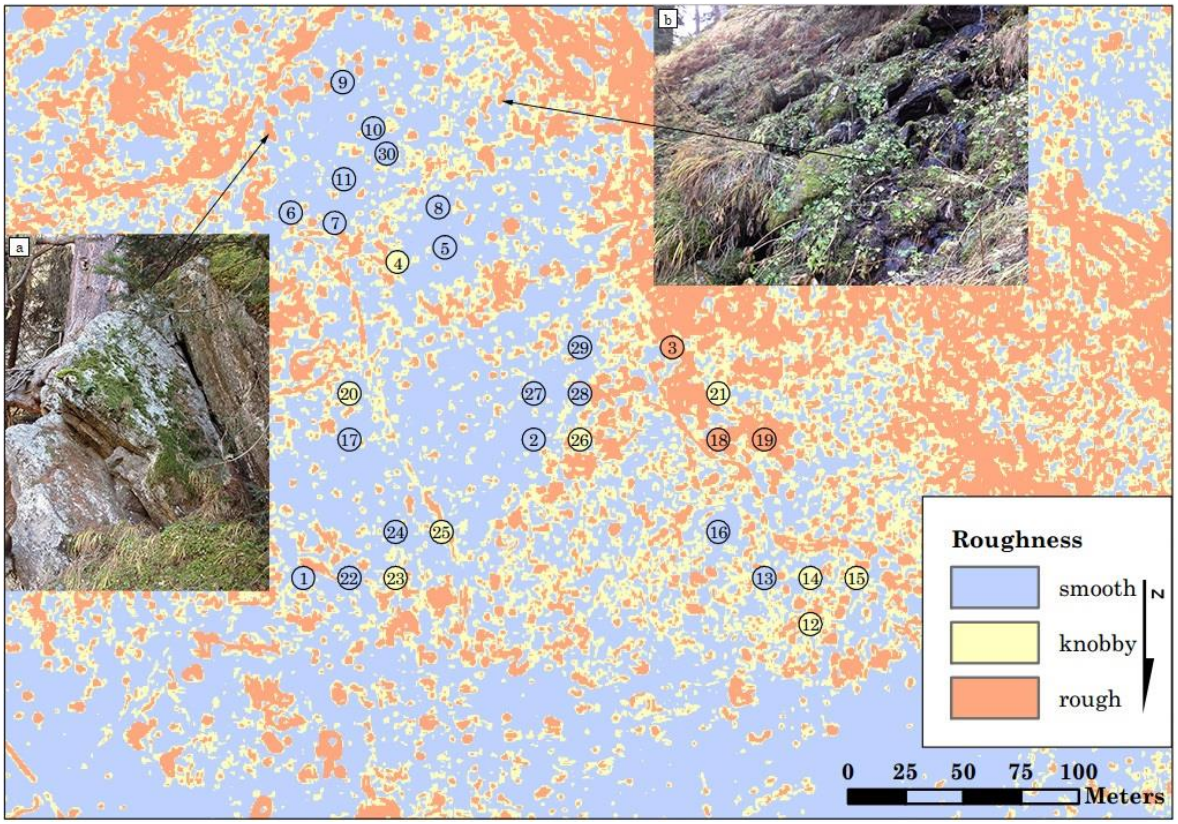

Figure 29: Terrain roughness derived from a DTM with 0.5 m resolution, classified into three classes with threshold values 0.01 and 0.02: smooth, knobby and rough. In all 30 sample plots, terrain roughness was classified according to calculated median value of the plot. Pictures a *and* b *show examples of rough terrain features.*

The terrain roughness derived from the DTM is classified smoother in comparison to the field observation (Figure 30). Roughness of sample plots classified in the field is distributed almost evenly in all three classes, with eleven sample plots in rough class (36.7 %), eleven in knobby class (36.7 %) and eight in smooth class (26.7 %). The distribution in the roughness classes derived from the DTM is following: three plots in the rough class (10 %), nine in the knobby class (30 %) and eighteen of the sample plots resulted to smooth class (60 %).

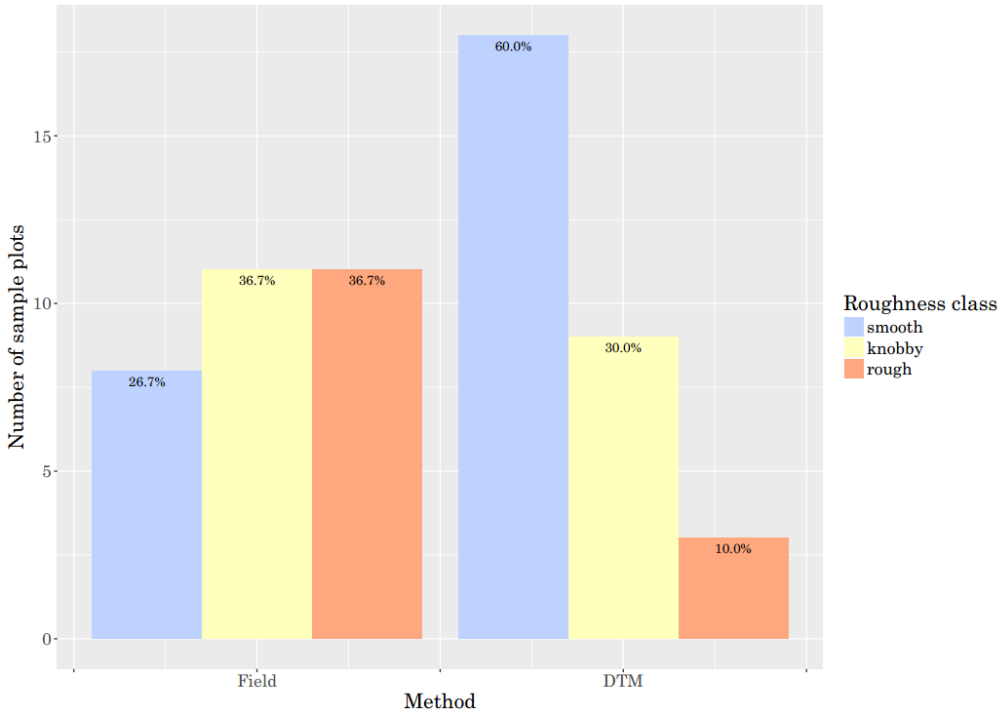

Figure 30: Distribution of sample plots in roughness classes using two methods of classification: in the field and from DTM.

The roughness derived from DTM differ from the roughness observed in the field (standard t-test shows significant difference with p-value < 0.05). From the total number of 30 sample plots, the terrain roughness derived from DTM matched with the field observation in 5 sample plots (17%). Most of the plots (40%) were classified one class smoother (8 plots are in the class smooth instead of knobby and 4 plots were classified as knobby instead of rough). 6 plots (20%) were classified as smooth, when in the field observed as rough. Another 6 plots were classified rougher by one class and 1 plot was classified as rough in comparison to the field observation, where it was classified as smooth (Table 7).

Table 7: Confusion matrix of modeled roughness derived from the DTM (prediction) compared to the observed roughness in the field (reference).

n = 30		Reference		
		smooth	knobby	rough
Prediction	smooth	**4**	**8**	**6**
	knobby	**4**	**1**	**4**
	rough	**1**	**2**	**0**

4.2.5 Diameter at breast height (DBH)

With increasing diameter at breast height (DBH), the height of a tree is increasing linearly all three tree species at Stillberg area (Pearson's positive correlation with p-value <0.001). Using RAMMS formula (Equation 3) for predicting DBH from height, DBH was calculated and compared to the actual measured DBH (Figure 31). The best prediction is for the Swiss stone pine, where the calculated DBH fits very well the actual measured DBH (standard t-test shows no significant difference). However, for mountain pine and larch, the calculated DBH varies from the measured DBH significantly (standard t-test shows significant difference with p-value <0.001 for both species).

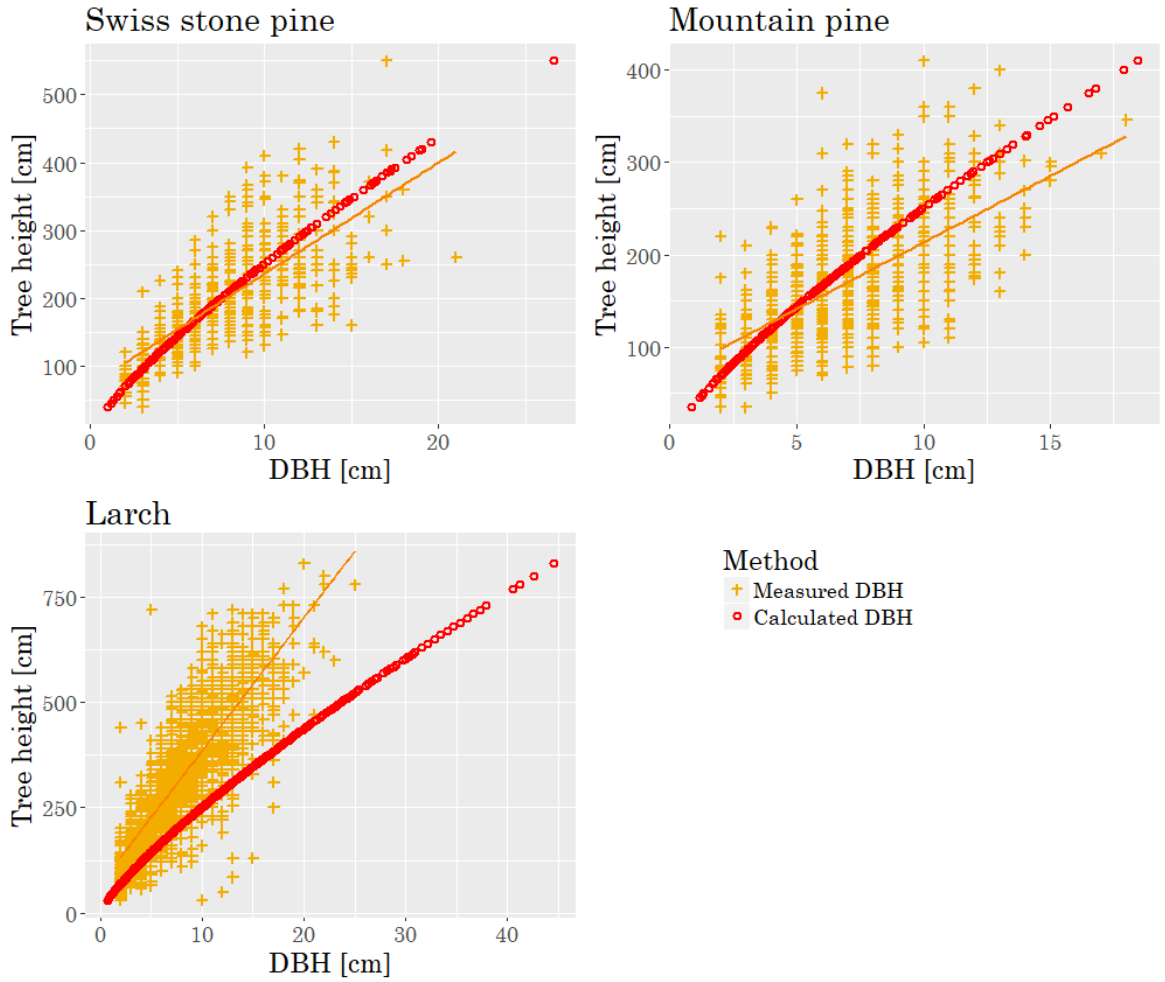

Figure 31: Comparison of measured and calculated DBH using formula from RAMMS (Equation 3). In the case of Swiss stone pine, calculated DBH represents the DBH well. However, in the case of mountain pine and larch, the calculated DBH varies from the measured DBH (Student's t-test shows significant difference with p-value <0.001 for both species).

4.2.6 K-values

The differences in K-values according to different remote sensing methods and the Field method are shown in Figure 32. The areas in the lower part of the avalanche track, with red shades, have negative difference, so the remote sensing methods underestimate the K-values. On the other hand, the areas in the upper part of the avalanche track with blue shades have positive difference that means that higher K-value was assigned to the remote sensing methods than to the Field method. Different shading was used to see the absolute difference, with darker shades for bigger difference.

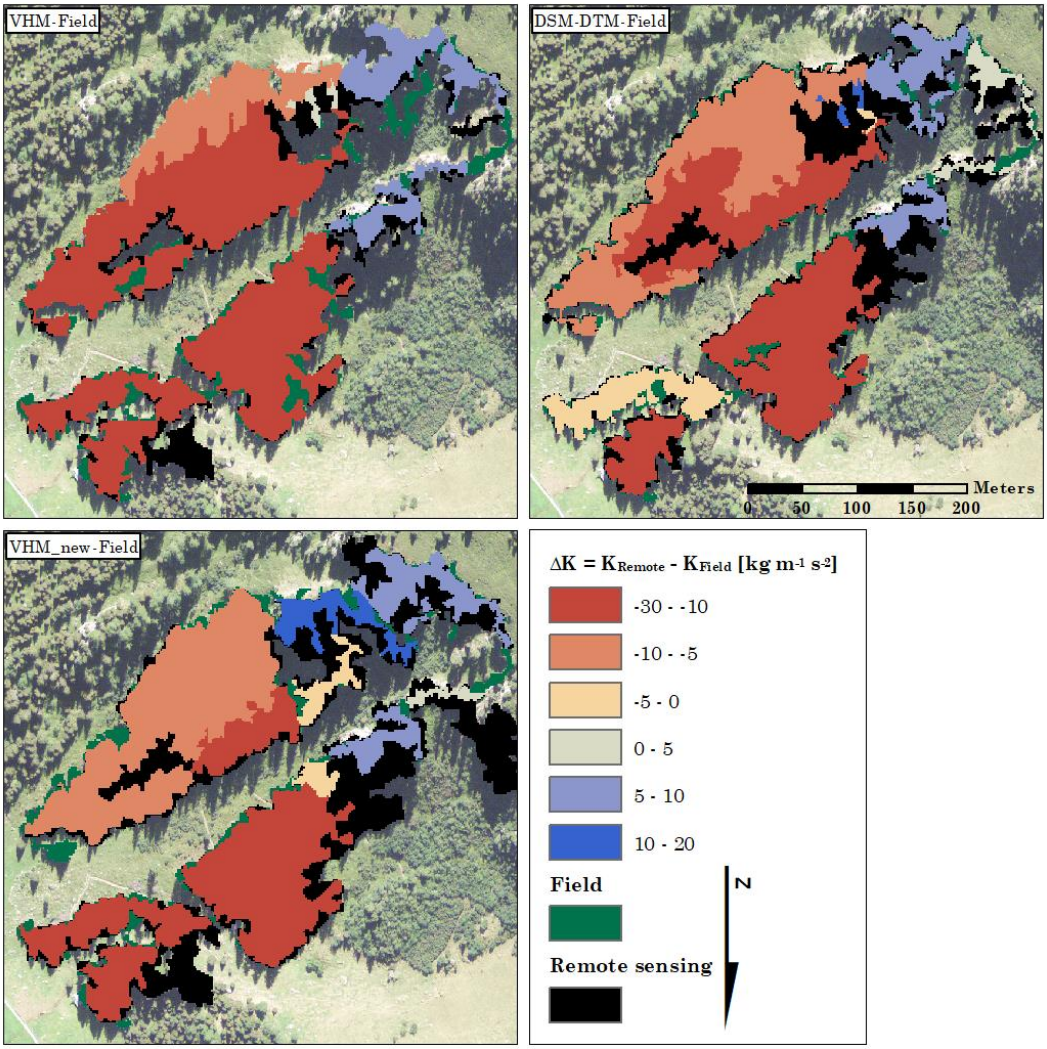

Figure 32: Difference in K-value for remote sensing methods and the Field method. The red shades show negative difference and blue shades show positive difference between the remote sensing methods and the Field methods. Areas detected only with the Field method are depicted in green colour and areas detected only with remote sensing methods are depicted as black.

Areas, which were not detected with the Field methods, but only with the remote sensing methods, are represented with black colour. The green areas were detected only with the Field method.

4.2.7 Simulation outputs from remote sensing methods

I simulated the avalanche from 2008 with present forest conditions using K-values assessed on four different methods: three remote sensing methods and a control Field method. Four very similar outputs resulted from the simulation of an avalanche with K-values assessed with field and remote sensing methods (Figure 33). In all four cases no forest destruction occurred. The remote sensing methods reproduced the runout distances very well, which are almost identical with some small deviation in the VHM and VHM_new. These have on the lower left side 3-4 m longer runout distance, with respect to the flow depth equal to zero.

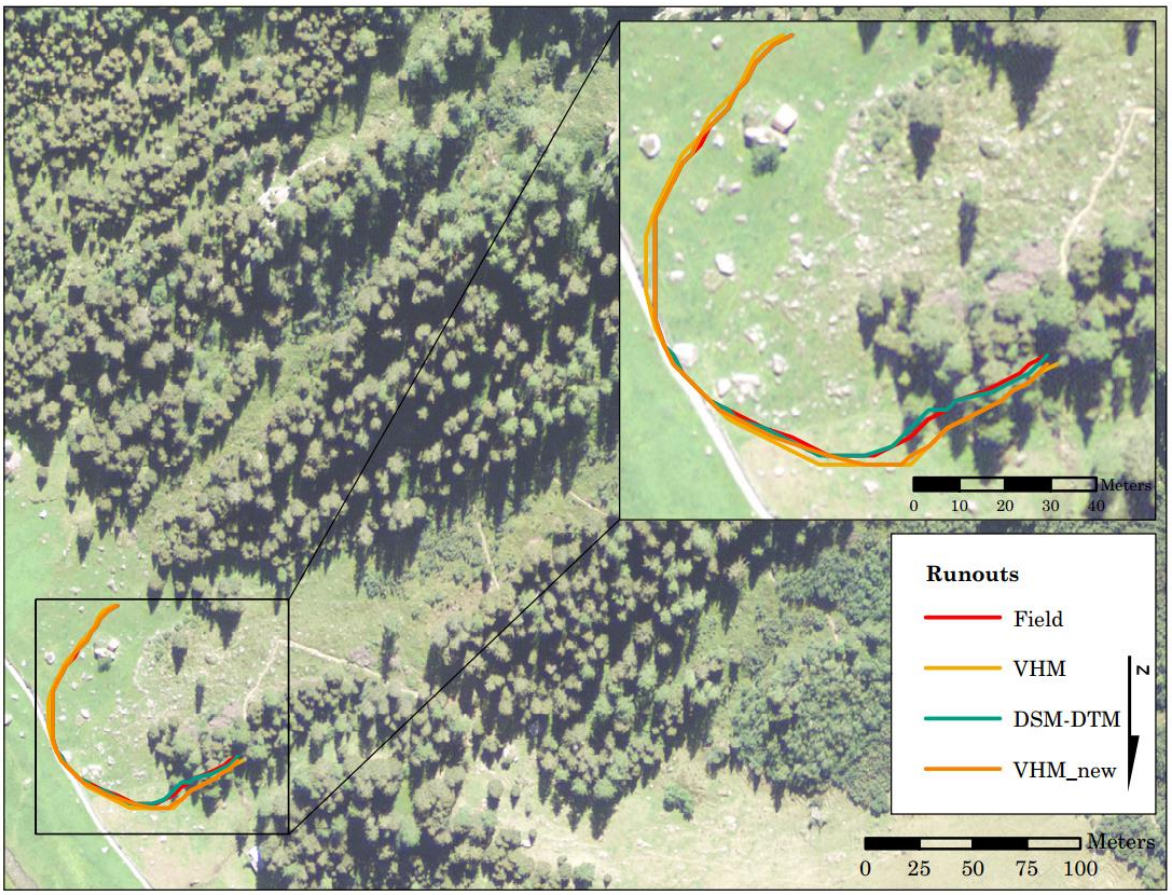

Figure 33: Resulting runouts of the field and remote sensing methods. The runout distances are very similar using different forest parameters assessed with these methods.

Comparing the maximum velocities, maximum pressure and maximum flow height, all four methods have similar results (Table 8), with the highest values for VHM method and the lowest values for VHM_new method. Considering the Field method as the control sample, the VHM is the most precise method with slightly overestimated results looking at the maximum values for velocity, pressure and flow height (Table 8). The difference in maximum velocity is 0.19%, in the maximum pressure 0.39% and the

maximum flow height 0.43% for the VHM method and the Field method. The methods DSM-DTM and VHM_new underestimate the resulting maximum values for velocity, pressure and flow height. The biggest differences in maximum values occur comparing the control Field method with VHM_new: maximum velocity differs by 0.28 m/s, maximum pressure by 4.72 kPa and maximum flow height by 0.06 m.

Table 8: Simulation results of the field and remote sensing methods: maximum velocity, maximum pressure and maximum flow height.

Method	Max velocity (m/s)	Max pressure (kPa)	Max flow height (m)
Field	21.09	177.88	2.30
VHM	21.13	178.57	2.31
DSM-DTM	20.97	175.84	2.28
VHM_new	20.81	173.16	2.24

4.2.8 Comparison to the avalanche from 2008

The avalanche in 2008 changed the forest structure and composition in the middle part of the avalanche track (Figure 34). Mainly younger spruce trees formed the forest composition in the middle part of the avalanche track before 2008. Nowadays, the green alder stand partly occupies this area. The avalanche in 2008 stopped in the lower part within the young forest. Using the same avalanche parameters, but the present forest information, the avalanche would result in longer runout distance.

The avalanche from 2008 has higher flow height only in the upper part of the avalanche track due to high forest detrainment within the forest in the middle and lower part of the avalanche track. The potential avalanche with present state of the forest has longer runout distance, high accumulation of snow also in the lower part and less detrainment due to lack of forest within the avalanche track, which was destroyed by the avalanche in 2008 (Figure 6).

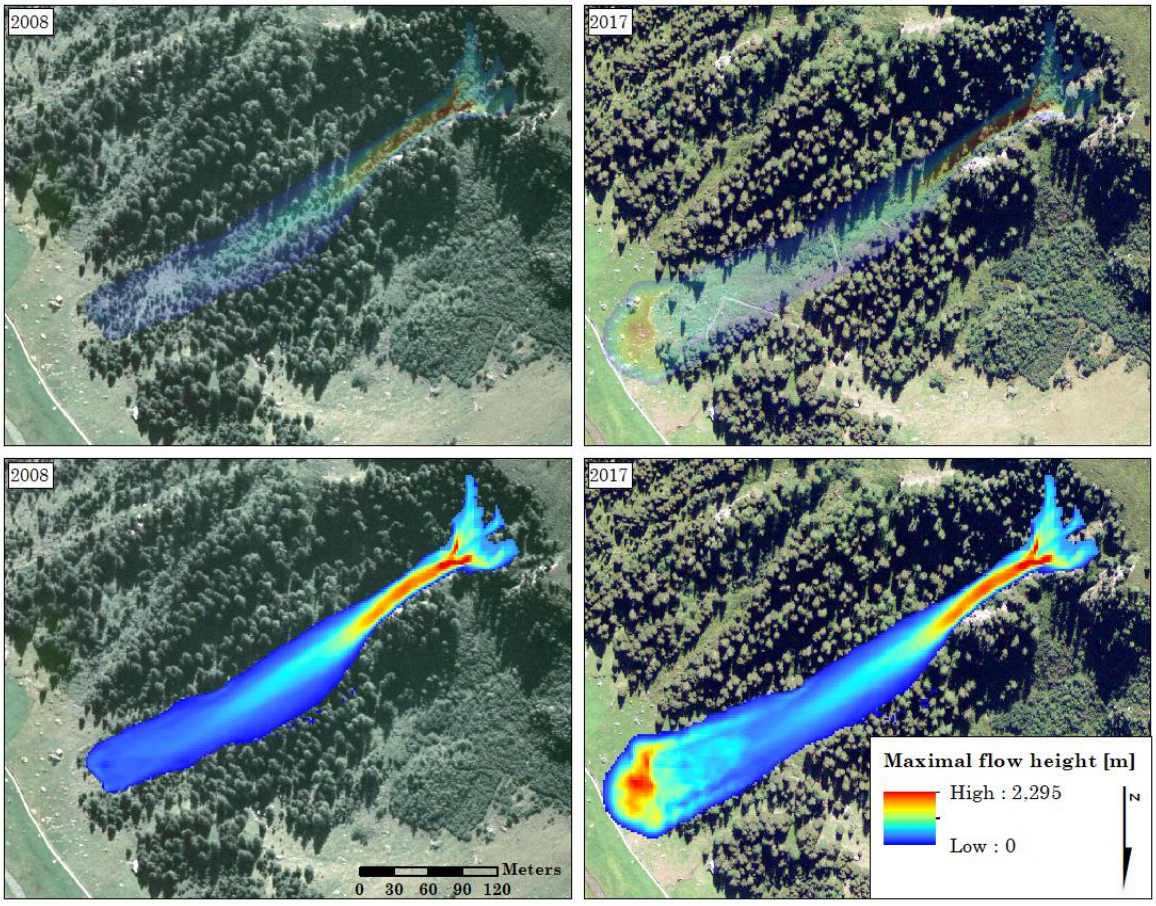

Figure 34: Maximal flow height of the avalanches from 2008 and a potential avalanche using forest condition from 2017. The avalanche from 2008 has shorter runout distance and higher flow height only in the upper part of the avalanche track; it is represented on the orthophoto from 2000. The avalanche using forest data collected in 2017 has longer runout distance and is represented on the orthophoto from 2016. Upper part is shown with transparency to show the forest change from 2008 to 2016.

4.3 Tree-snow interaction in the initial stages of forest succession

4.3.1 Maximal snow height and number of trees

At the area of Stillberg afforestation, the number of trees within the plots was tested with correlation analysis against the corresponding lath values for maximal snow heights in several winter seasons (1975, 1979, 1982, 1985, 1990, and 1995). The maximal snow height and number of trees are not correlated in 1975, 1979 and in 1982. After 10 years of afforestation (1985) we can observe the influence of trees. With increasing number of trees, maximal snow height decreases (negative correlation with high significance with correlation value -0.2 and *p*-value 0.001; Figure 35). This relation between number of trees per plot and the maximal snow height is the same in the following years (even stronger negative correlation in 1990 with correlation value -0.3 and *p*-value <0.001, in 1995 with correlation value -0.2 and *p*-value 0.008; Figure 36 and Figure 37). Fitting the linear model, all three cases are rather scattered with r^2 equal to 0.07, 0.14 and 0.04 in the years 1985, 1990 and 1995, respectively.
Looking at the three tree species (European larch, Swiss stone pine and mountain pine) separately, all have the same influence on the maximal snow height within the plots. From the year 1985 on, with more trees on the plot, there is decreasing snow height (Pearson's negative correlation is significant from the year 1985 on).

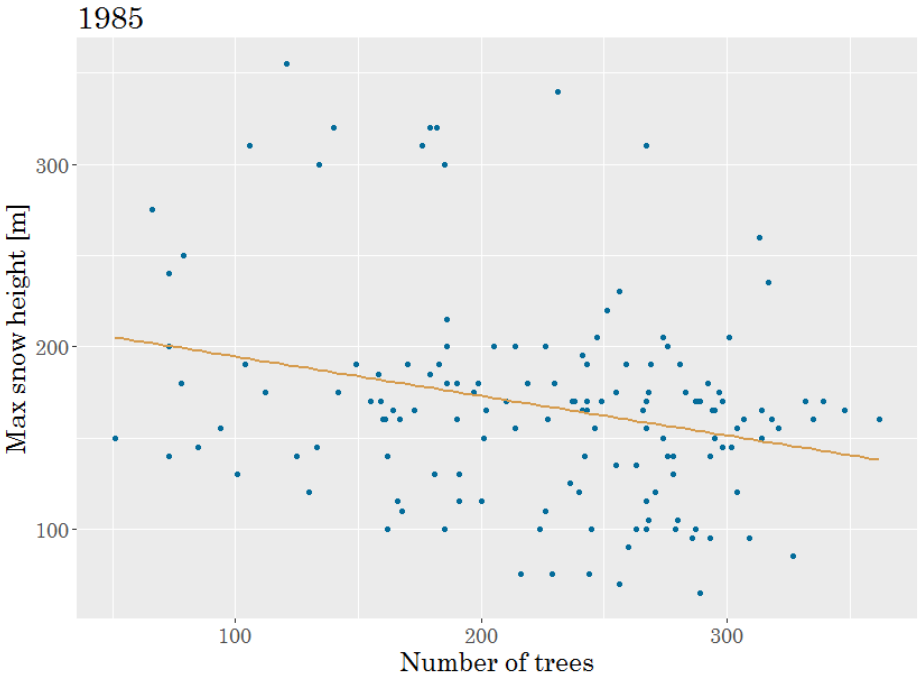

Figure 35: Linear relationship between the maximal snow height and number of trees per plot in 1985, r^2=0.07. Correlation analysis shows strong negative correlation.

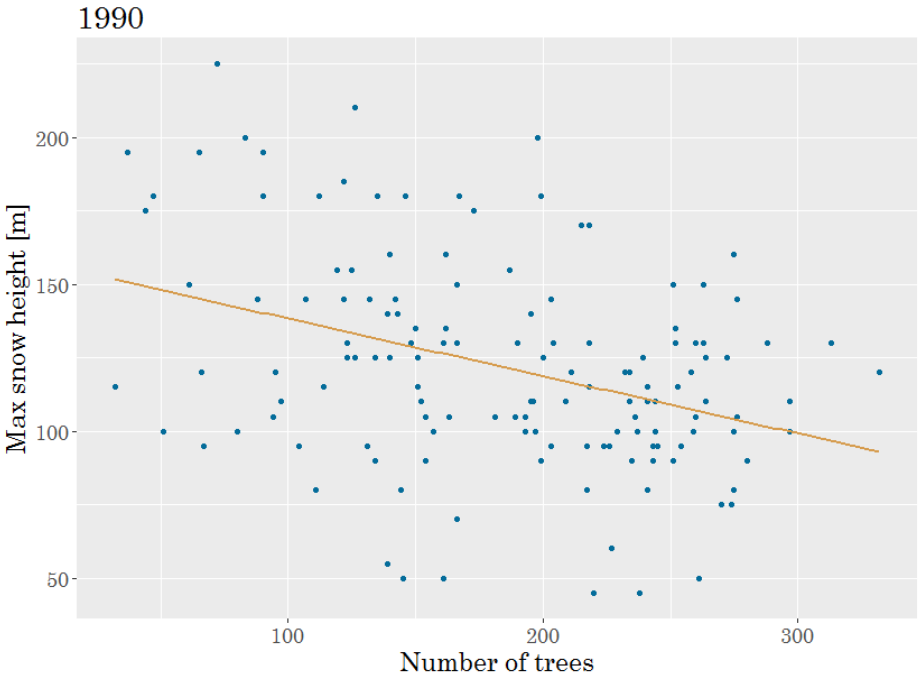

Figure 36: Linear relationship between the maximal snow height and number of trees per plot in 1990, r^2=0.14. Correlation analysis shows even stronger negative correlation than in 1985.

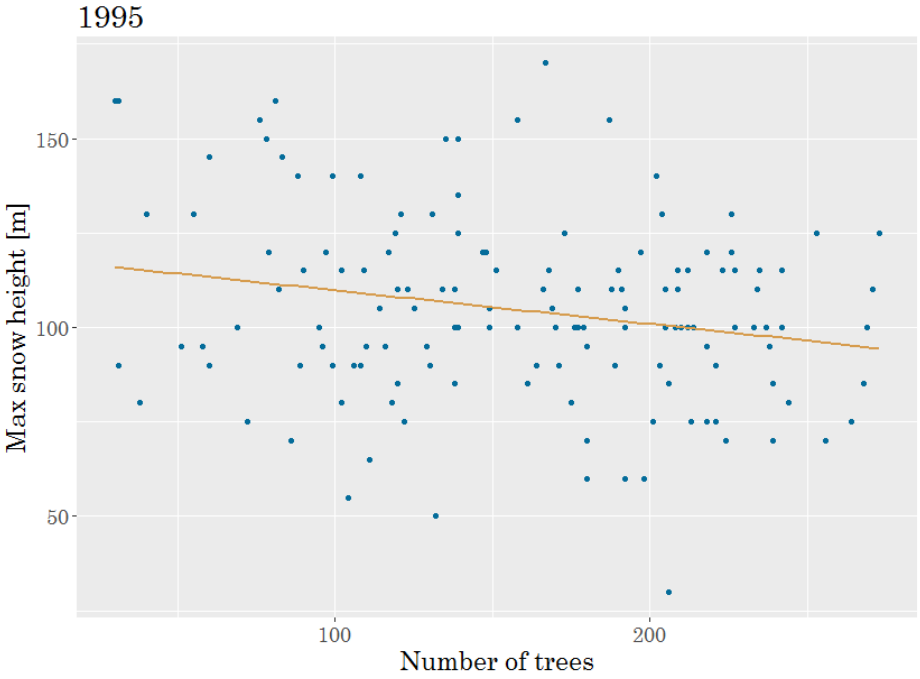

Figure 37: Linear relationship between the maximal snow height and number of trees per plot in 1995, r^2=0.04.

In the year 1985, mean number of trees per plot was 226, which means 11 530 trees per hectare. The number of trees during time was decreasing, in 1990 the mean number of trees per plot was 187 (= 9 541 trees per hectare) and in 1995 the mean number of trees per plot was 158 (= 8 061 trees per hectare).

4.3.2 Maximal snow height and elevation, dominant tree height

To confirm the hypothesis that the number of trees influences the maximal snow height as a main factor, elevation has to be tested. The maximal snow height at different plots was tested with correlation analysis against the elevation of these plots. No significant correlation was found (in the years: 1975, 1979, 1982, 1985, 1990, 1995).

The maximal snow height and the dominant tree height (mean of the three highest trees per plot) were tested for correlation, testing also all three tree species separately, but no significance in any of the tested years (1975, 1979, 1982, 1985, 1990 and 1995) was discovered.

4.3.3 Tree height and number of avalanches

With increasing tree height number of avalanches is decreasing and after 2011 no more avalanches occur at Stillberg afforestation. The relation between decreasing number of avalanches and increasing tree height (Figure 38) were tested and the result shows strong negative correlation (with correlation value -0.8 and *p*-value 0.01677).

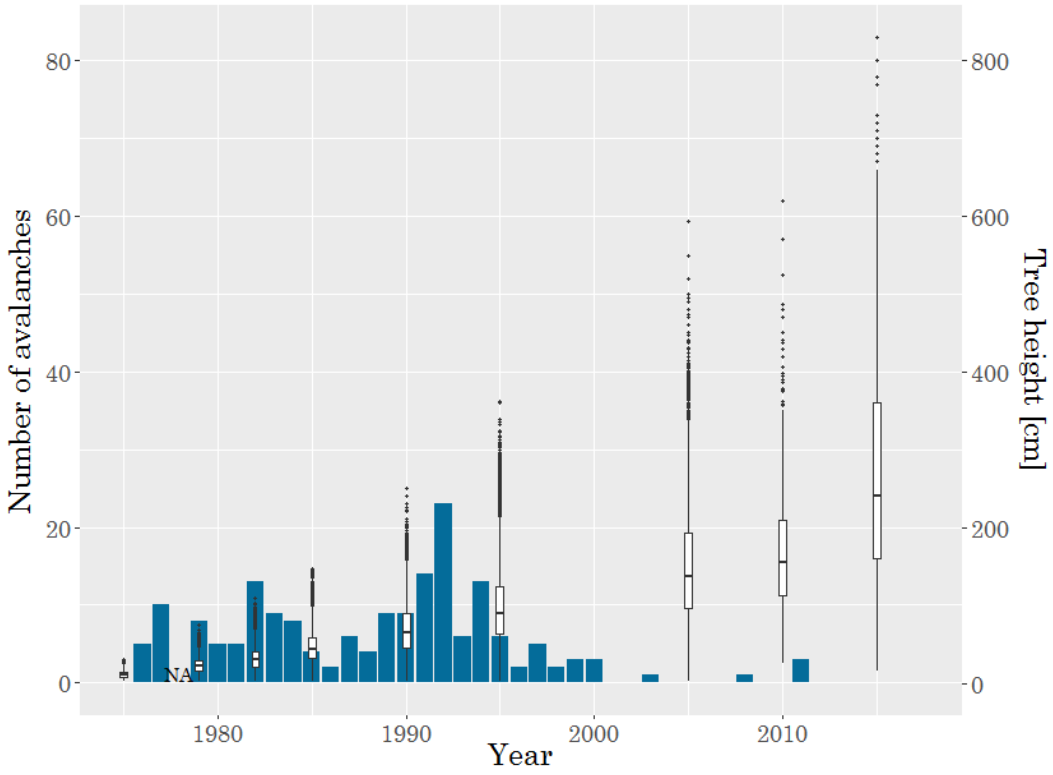

Figure 38: Number of avalanches at studied part of Stillberg and increasing tree height.

4.3.4 Number of avalanches at Stillberg

The number of mapped avalanches at the part of Stillberg without snow bridges is decreasing. The overall mean (from 1976 to 2017) of mapped avalanches is 4.37 avalanches per year. In the last 20 years (1997-2017), the average sinks to 0.86 avalanches and even less avalanches occur in the last 10 years (2007-2017), in average 0.36 avalanches per year (Figure 39). The highest occurrence of avalanches at this part of Stillberg was in the winter 1991/1992 with 23 mapped avalanches. The graph from the whole Stillberg afforestation also illustrates the decreasing trend in avalanche occurrence from 1959 to 1994 (Figure 40).

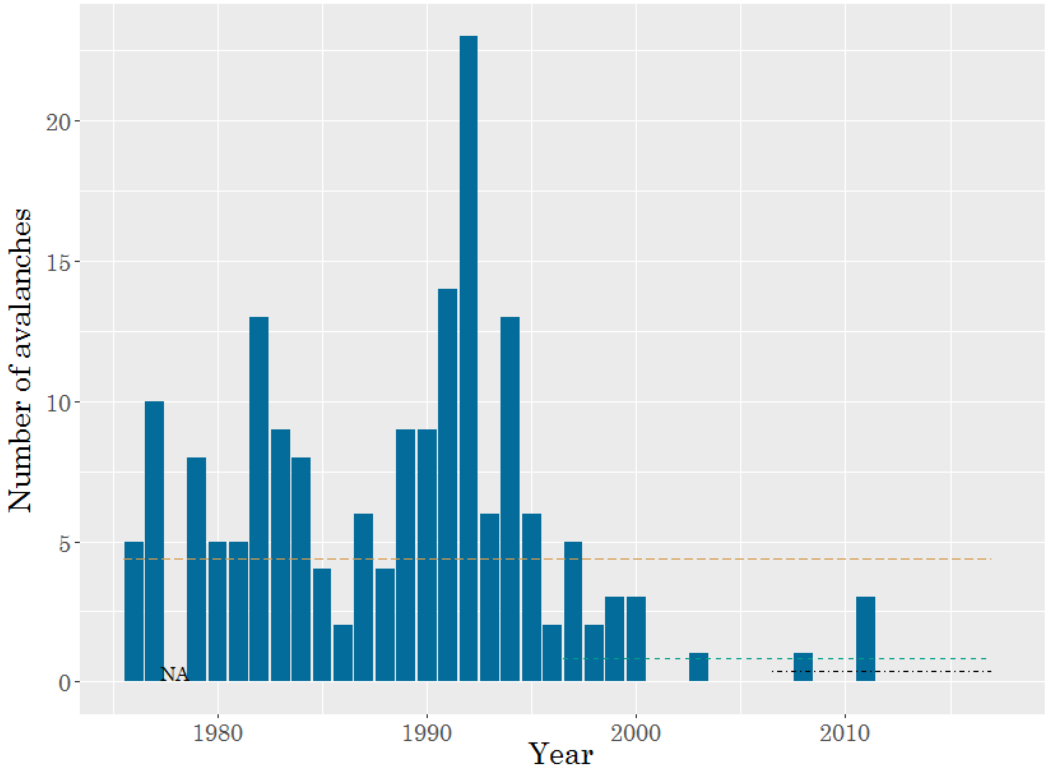

Figure 39: Number of mapped avalanches at studied part of Stillberg and overall mean (4.37, yellow dashed line), mean from last 20 (0.86, green dashed line) and 10 years (0.36, black dot-dashed line).

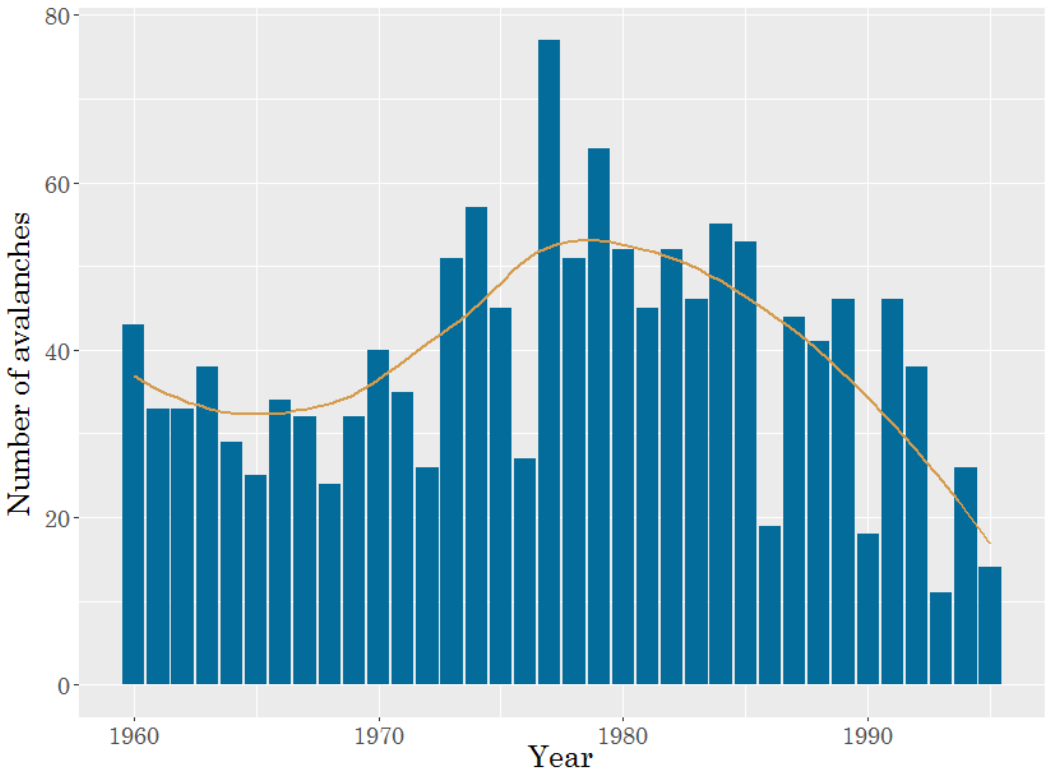

Figure 40: Number of avalanches in at the whole Stillberg area from 1959 to 1994, with decreasing trend over last 15 years.

5 Discussion

5.1 Avalanche simulation with varying release and forest areas

Using the available information from the observed avalanche at Teufi in 2008, various simulation parameters were tested. The most matching release area, with respect to the direction and runout distance, have stauchwall at the inclination change and does not include trees within the area. After choosing the optimal release area according to the most similar runout as the avalanche from 2008, it was necessary to consider the green alder stands. Green alder was tested within the simulation as forest stand (using K-value 15 and tree species birch), which produced shorter runout. Looking at the forest destruction, which also happened within the green alder stand, this does not represent the reality well. Avalanches disturb the green alder rarely; it can outlast snow cover, gliding snow and avalanches well and it is usually bended under the weight of the snow (Aley, 1960; Hug, 2013). The impact of green alder on snow avalanche formation is less clear. Some authors claim the negative influence of green alder on the snowpack and that the suppressed branches create gliding surface for snow and avalanches (Aley, 1960; Hug, 2013). The green alder hinders forest succession and therefore does not offer the same avalanche protection as the montane forest (Bühlmann et al., 2014). Other authors believe that even though the green alder is often buried under the snow, it has the ability of stabilizing the snowpack by increasing the surface roughness and thus the basal friction (Poncet, 2004). This was tested by sensitivity analysis using different values for friction parameter Xi, resulting in more realistic outputs. Green alder should be handled in RAMMS as a special forest type next to the evergreen/mixed and larch/deciduous with decreased detrainment, but increased friction; or as an additional friction area.

Similarly, Sitko (2008) has categorized forest types for release probability using remote sensing data. He classified forests into three categories: next to the evergreen and deciduous forest types as in RAMMS, he added dwarf mountain pine (*Pinus mugo).* Crown coverage was considered as the most important factor in combination with forest type and surface roughness. The highest capacity in mitigating the release of avalanches has the evergreen forest with very dense crown coverage. The deciduous forest with the maximum crown coverage never reaches zero probability of release. Interestingly, by mountain pine, release probability increases with crown coverage

more than 80%. In the case of higher snow cover, dwarf mountain pine with 100% crown coverage creates suitable sliding surface for initiating avalanches (Sitko, 2008).

5.1.1 Destructive pressure

Forest destruction according to the simulation takes place only in the upper part of the avalanche path; however, it is underestimated in the lower part, as in Feistl et al. (2015). Values included in the RAMMS thresholds for tree breakage vary significantly from the values found in Peltola et al. (2000). I tested the most realistic approach (Feistl et al., 2015) for calculating the destructive pressure, using the sliding block model (SBM). The calculated bending stress of the lower part of Teufi avalanche (39.6 MPa) was compared to the values of bending strength used also in Feistl et al. (2015), which according to Peltola et al. (2000) is for spruce 36 MPa (RAMMS value 72 MPa) and for larch 37 MPa (RAMMS value 109 MPa). Trees break if the calculated bending stress overcomes the bending strength of the trees, which occurs when using the avalanche volume length l_v = 20 m and longer.

5.1.2 Forest scenarios

The scenario without forest overestimate the runout distance (60 m longer compared to the avalanche from 2008) and it stops only due to the increasing flat terrain in the area of the hiking path. Observing the impacts of largescale harvesting brought more focus on the forest's protective effects already hundreds years ago, when the colonization of the Alps began (Brang et al., 2001). The importance of vegetation coverage in hindering the avalanche flow is high. Clearcutting may thus have an important influence on avalanche initiation; it creates new potential release areas for avalanches (McClung, 2001; Breien and Høydal, 2012). According to the scenario with dense forest øust below the release area, runout distance shortens by 50 m and the scenario with forest in the avalanche track, runout distance shortens by 80 m with respect to the runout distance of an observed avalanche. In Teich et al. (2012b), the avalanches that started higher up from the forest had longer runout distance. The resulting shorter runout distance with forest in the avalanche track could be the effect of the length of the potential dense forest area, which is longer in the scenario #3 than in the scenario #2. The distance through the forest is essential and a long travel distance through forest leads to shorter runout distance (Teich et al., 2012b). However,

the efficiency of the forest's resistance depends not only on the distribution and size of the trees, but also on the avalanche size and slope angle (Schneebeli and Bebi, 2004). The slope in the upper part of Teufi avalanche is very steep and afterwards decreases. In the scenario with dense forest located right below the release area (scenario #2), avalanche enters the forest on the steep slope, the velocity increases and the forest does not affect the avalanche runout as remarkably as in the case of the scenario #3 with dense forest in the avalanche track. There, the velocity is already decreasing due to the decreasing slope inclination and the forest affects the runout of the avalanche more considerably. The snow detrainment reduce the velocity and this affects the runout distance as well (Feistl et al., 2014). The scenario #3 has more detrainment behind trees and has thus shorter runout distance than scenario #2.

5.2 Comparison of field and remote sensing measuring methods

5.2.1 Creating forest polygons

Forest and green alder polygons were manually established according to the forest type and the crown coverage. Only some of the methods detected green alder areas. These are mainly shaded places, which in case of Field method, DSM-DTM or VHM_new were more or less detected resulting in creating polygons with green alder. In case of VHM shaded places caused problems in height detection and no green alder polygon is available. The original VHM did not detect some of the high elevation evergreen trees with narrow crowns due to the lower spatial resolution of the aerial images of 0.5 m (Ginzler and Hobi, 2016), so the correction was implemented (VHM_new). In the case of VHM_new, forest variability was smoothened and only few big polygons were created. The correction of the original VHM is well visible on the example of Teufi, where the VHM_new overestimates the forest cover and no forest gaps are detected. This could be problematic for avalanche simulations, since the forest gaps, depending on slope, crown cover density and the size of the gaps, are prone for avalanche release (Schneebeli and Bebi, 2004).

The most precise estimate is delivered by the DSM-DTM method, which detects also the shaded areas within the forest stand, which are hard to classify from the orthophoto.

5.2.2 Maximal tree height

Teufi and Stillberg

No significant differences were found in the remote sensing measuring methods when counting with all 30 sample plots. However, looking separately at the methods with regard to forest types (Dense forest, Open forest and Green alder) the DSM-DTM method (difference between the digital surface model and the digital terrain model) differs from the Field method within the group of Open forest. In Open forest more structural variability occurs as in Dense forest and the difference in measuring methods could be caused by including bordering trees. The buffer of 5 m radius is rather small and the problematic parts are the branches of bordering trees included in the digital data. Field method is including trees, which were intersecting with this radius with their stem only and does not include bordering trees intersecting only with their

branches. This does not occur in the group Dense forest, where, expecting homogeneous forest stand, only the highest top counts.

Testing the same four methods at the Stillberg afforestation, the DSM-DTM differs from the other methods. This method overestimates the maximal heights within this area. The both vegetation height models (VHM and VHM_new) represent the measured height well.

5.2.3 Roughness

The terrain roughness is smoothened when using the predicted roughness from DTM in comparison to the field observation. Predicted roughness is rather smooth (60% of sample plots) and only 10% of the sample plots are defined as rough in comparison to the field observation, where 26.7% of sample plots classified as smooth and 36.7% as rough. Small-scale topographic roughness can have big influence on the avalanche flow, which in case of Sovilla et al. (2012) has changed the expected direction of the wet-snow avalanche. In the case of faster avalanche the same topographic roughness may have deflected the avalanche away from the dam (Sovilla et al., 2012). Bühler et al. (2011) suggest using high resolution and quality DTM including any relevant terrain roughness as an input for the avalanche simulations.

5.2.4 DBH-height

RAMMS uses simple formula for height estimation, where height is equal to $DBH^{0.8}$ (Equation 3). Testing this formula on trees at Stillberg area by comparing the measured DBH and the DBH calculated from the RAMMS formula, this formula is not precise for different tree species. It is reliable in predicting DBH for the Swiss stone pine, however, the calculated DBH does not match with the measured DBH for mountain pine and larch. After different literature (Sterba, 1976; Omule, 1984; Eckmüllner, 1985), there are many models for DBH-height, and the relationship varies among different characteristics as tree species, tree age, site characteristics and management (Omule, 1984). RAMMS could be improved by including different models for the relationship between DBH-height for different tree species or include both DBH and height as input data to exclude the calculation procedure.

5.2.5 K-values

All three remote sensing methods (VHM, DSM-DTM and VHM_new) underestimate the K-values in the middle and lower part of the avalanche track, comparing them to the field method. The surface roughness has a big influence on the resulting K-value. According to the different roughness class, K-value varies of 10 from smooth to knobby and from knobby to rough (e.g. K-values: 28 for smooth, 38 for knobby and 48 for rough class). In the upper part of the avalanche track, forest is more open and surface is very rocky, here is probable that the surface roughness is well estimated or even overestimated, which has an influence on the K-value.

5.2.6 Simulation outputs

Three remote sensing methods (VHM, DSM-DTM and VHM_new) were tested on the avalanche from 2008 using the present forest information. Field data served as control method. Resulting outputs were very similar comparing the runout distance, maximum velocities, maximum pressure and maximum flow height. The best prediction of runout distance is delivered by the DSM-DTM method and only small deviations on VHM and VHM_new occurred. VHM and VHM_new methods overestimated the runout distance by only 3-4 m. The VHM method delivers the most precise values for maximum velocity, maximum pressure and maximum flow height. The DSM-DTM and VHM_new underestimate the maximum values for velocity, pressure and flow height.

5.2.7 Comparison to the avalanche from 2008

The avalanche at Teufi in 2008 created forest destruction in the avalanche path (Figure 6), which is also visible comparing the orthophoto from 2000 before the avalanche happened and an orthophoto from 2016 with current state of the forest (Figure 34). The most common impacts of avalanche activity are lower tree age and size, higher share of deciduous species, higher shrub and herbal cover (Vacchiano et al., 2015). As in the case of avalanche track at Teufi, the forest structure and composition changed completely from young spruce forest towards green alder.

Comparing the runout distance of the original avalanche from 2008 and the distance of the potential avalanche using present forest information, less forest cover leads to less

forest detrainment and longer runout distance. When the disturbance is frequent or substantial, a forest is unable to establish and create essential protection. It is unable to establish or it is constantly disturbed in an early successional stage as in the case of avalanche tracks (Johnson, 1987).

5.3 Tree-snow interaction in the initial stages of forest succession

The Stillberg afforestation, the largest and the longest lasting experiment on drivers of ecological processes at treeline, offers unique database for the study of vegetation-snow interactions. In the 1975, 92 000 trees were systematically planted, which were then observed and measured. Already before the afforestation from the winter 1959/1960, snow height at the snow laths and avalanches were monitored (Bebi et al., 2009b).

5.3.1 Maximal snow height and number of trees

The available data from trees measurements (from years 1975, 1979, 1982, 1985, 1990, and 1995) were used to test the influence of these trees on the maximal snow height. The Stillberg area was divided into plots around the snow laths, where snow height was measured and number of trees within these plots counted. After 7 years from planting, only 74% of the trees at Stillberg survived and the trees were still too small, mostly less than 50 cm high (Bebi et al., 2009b). No influence of the number of trees on snow height was observed. However, after 10 years of afforestation (in 1985), there is significant influence of number of trees on the maximal snow height. As more trees on the plot occur, there is lower maximal snow height. This applies to the tree species separately as well, all tree species show negative correlation between number of trees at the plot with the maximal height of snow.

Number of trees (per hectare, also in terms of density of a forest cover) is regarded as an important structural parameter influencing the release of avalanches (Schneebeli and Bebi, 2004; Viglietti et al., 2009). In the year 1985, mean number of trees per plot were 226, which means 11 530 trees per hectare. The number of trees during time was decreasing, in 1990 the mean number of trees per plot was 187 (= 9 541 trees per hectare), in 1995 the mean number of trees per plot was 158 (= 8 061 trees per hectare). These values are hard to compare with other literature, since there is no information about the DBH available and most of the values for number of trees per hectare are connected with bigger DBH. In the 1982, most of the trees were smaller than 50 cm and the mean height in 1995 was 97 cm, thus it is not possible to calculate the DBH. For an overview, Ishikawa et al. (1969) published following values for slope of 45° and DBH = 5 cm, number of trees per hectare should be over 10 000. Other literature shows values mainly for mature forest and not for the initial stages.

Due to the continuous growth of trees, snow precipitation is unevenly deposited in comparison to the open land. The trees intercept some of the snow (Schneebeli and Bebi, 2004) and this influence the measurements of the maximal snow height during the season. After 10 years of afforestation, interception plays more important role than before. Where more trees occur within the plot, interception rates are higher and this leads to lower maximal snow heights. Snow interception influence the snowpack within a distance of about 1.5 m times the crown projection for mature trees (Schneebeli and Bebi, 2004). In the future, we can expect less trees, but increasing interception due to larger crown coverage.

5.3.2 Maximal snow height and elevation, dominant tree height

The maximal snow height can differ according the elevation, where in the lower parts less snow occur in comparison to the higher places. More snow precipitation occur at higher elevation, however, snow heights are also influenced by the wind (Grünewald et al., 2014). The maximal snow height at different plots was tested against the elevation to exclude the elevation as an influencing factor. In the years 1975, 1979, 1982, 1985, 1990 and 1995 did not show any significant relation between the maximal snow height and the elevation.

The maximal snow height at different plots was tested for correlation against the dominant tree height (mean of the three highest trees per plot). No significance in any of the tested years was found for all the tree species together or separately.

5.3.3 Tree height and number of avalanches

The influence of growing trees on avalanches at Stillberg area is evident. With increasing height of the trees, less avalanches take place and after the year 2011 no more avalanches occur. Since the 19th century in many areas of the Alps forest expanded, mostly in the steep slopes above 30°, and the avalanche activity decreased (Bebi et al., 2009a).

5.3.4 Number of avalanches at Stillberg

The influence of the trees is clearly visible on the number of avalanches which were recorded at Stillberg. The total number of avalanches is decreasing at the studied part of Stillberg without the snow bridges as well as at the whole area of Stillberg. The trees hinder the formation of snow avalanches already after 36 years after the afforestation. Not only the crown coverage and interception have an influence on hindering avalanches within a forest stand (Frey, 1977), but also the tree stems with so-called back-pressure zones play role in stabilizing the snowpack. Likewise in the dense forest, gliding snow is not to be expected. Glide-snow avalanches occur on smooth ground, so the number of trees per hectare and the roughness of the surface are important features in preventing the avalanche release (Schneebeli and Bebi, 2004; Höller, 2017). Areas without trees should be included in the next research to compare the development of the total number of avalanches outside the Stillberg to verify the forest influence.

6 Conclusions

With increasing size of the release volume, the runout of avalanche becomes longer, thus it is important to choose the release area carefully. In my case, the optimal release area was chosen according to the inclination change, where the stauchwall was set and did not include trees within the area. Forest structure parameter (K-value) influences runout distance and forest destruction. The problematic part in this study was the green alder stand (as well as it could be dwarf mountain pine stand) and this should be included as a special group in the simulations. More research in this direction is essential to quantify the effect of these particular forest stands on avalanches.

Due to underestimated forest destruction, the present thresholds for tree breakage included in RAMMS should be reconsidered. With more study cases of observed forest destruction, this could be improved.

The remote sensing methods (as VHM or DSM and DTM) are suitable for determination of forest parameters (K-value), which enter the avalanche simulation in RAMMS. The simulation outputs (using the information from the remote sensing methods) are very accurate comparing them to the control method (data obtained in the field), even though single forest characteristics as height or surface roughness slightly differ, it has almost no influence on the resulting runout distance of the avalanche (±3-4 m). The DTM in combination with the current VHM, which is now available for whole Switzerland, can be applied in avalanche simulations.

I would like to propose including the tree height directly as input in RAMMS, as some smaller inaccuracies could occur by calculating the height from DBH using one equation for all different tree species and ages. In the case of missing information on one of the two parameters (DBH or height), it would be possible to calculate the missing one by including simple form factor equation (e.g. Pollanschütz model) for single tree species with corresponding DBH or height.

The influence of the growing trees in the initial successional stage is evident; it effects positively the snowpack stability through increasing interception, and it prevents avalanche release. At the Stillberg afforested area, where the avalanches periodically released, no more avalanche activity was observed more than 36 years after

the afforestation. The next step is to compare these results to a control site without trees next to the Stillberg afforestation, to confirm the influence of the vegetation.

Bibliography

Aley, T.J., 1960. Snow Avalanche Tracks and Their Vegetation. Master thesis. University of California, 52 p.

Ancey,C., 2008. Chapter 13: Snow Avalanches. Geomorphological Fluid Mechanics. Lecture Notes in Physics. Vol. 582, 319-338.

Baggi, S., Schweizer, J., 2009. Characteristics of wet-snow avalanche activity: 20 years of observations from a high alpine valley (Dischma, Switzerland). Natural Hazards 50 (1), 97-108.

Bartelt, P., Bühler, Y., Christen, M., Deubelbeiss, Y., Salz, M., Schneider, M., Schumacher, L., 2013. RAMMS. User Manual v1.5 Avalanche. WSL Institut für Schnee- und Lawinenforschung SLF, Davos, 97 p.

Bebi, P., Kulakowski, D., Rixen, C., 2009a. Snow avalanche disturbances in forest ecosystems - State of research and implications for management. Forest Ecology and Management. 257(9), 1883-92.

Bebi, P., Hagedorn, F., Rixen, C., Senn, J., Wasem, U., 2009b. Forschung am Stillberg vor 25 Jahren und heute. Inf.bl. Wald 25, 5-7.

Brang, P., Schönenberger, W., Ott, E., Gardner, B., 2001. 3: Forests as Protection from Natural Hazards. In: Evans J., 2001. The Forests Handbook. Volume 2. Applying Forest Science for Sustainable Management. Wiley-Blackwell, 816 p.

Breien H., Høydal Ø. 2012. Influence of Forest on Snow Avalanche Hazard - Norwegian Challenges. Proceedings ISSW, 633-638.

Bründl, M., Margreth, S., 2015. Chapter 9: Intergative Risk Management: The Exmaple of Snow Avalnches. Snow and Ice-Related Hazards, Risks and Disasters, 263-301.

Bundesrepublik Österreich, 1975. Forstgesetz BGBl. Nr. 440/1975: ForstG.

Bühler, Y., Christen, M., Kowalski, J., Bartelt, P., 2011. Sensitivity of snow avalanche simulations to digital elevation model quality and resolution. Ann. Glaciol., 52, 72-80.

Bühler, Y., Kumar, S., Veitinger, J., Christen, C., Stoffel, A., Snehmani, 2013. Automated identification of potential snow avalanche release areas based in digital elevation models. Nat. Hazards Earth Syst. Sci., 13, 1321-1335.

Bühlmann. T., Hiltbrunner, E., Körner, C., 2014. Alnus viridis expansion contributes to excess reactive nitrogen release, reduces biodiversity and constrains forest succession in the Alps. Alp Botany, 124, 187-191.

Christen, M., Kowalski, J., Bartelt, P., 2010. RAMMS: Numerical simulation of dense snow avalanches in three-dimensional terrain. Cold Regions Science and Technology 63 (1-2), 1-14.

Crawley, M. J., 2007. The R Book. John Wiley & Sons Ltd., 942 p.

de Quervain, M., 1978. Wald und Lawinen. Proceedings IUFRO Seminar Mountain Forests and Avalanches, Davos, 219–231.

Eckmüllner, O. 1985 Einheitshöhenkurven und Alters-Höhen-Durchmesser Funktionen für Fichte und Buche im Lehrforst. Diploma Thesis, University of National Research and Applied Life Science, 66 p.

FAO, 1998. FRA 2000 Terms and Definitions. FAO, Rome, Italy.

FRA, 2000. Global Forest Resources Assessment 2000. Main report. FAO, Rome, Italy.

Feistl, T., 2015. Vegetation effects on avalanche dynamics. Dissertation. Technische Universität, München. 124 p.

Feistl, T., Bebi, P., Christen, M., Margreth, S., Diefenbach, L., Bartelt, P., 2015. Forest damage and snow avalanche flow regime. Natural Hazards and Earth System Science 15 (6), 1275–1288.

Feistl, T., Bebi, P., Teich, M., Bühler, Y., Christen, M., Thuro, K., Bartelt, P., 2014. Observations and modeling of the braking effect of forests on small and medium avalanches. Journal of Glaciology 60 (219), 124–138.

Frey, W., 1977. Wechselseitige Beziehung zwischen Schnee und Pflanze – eine Zusammenstellung anhand von Literatur Mitteilungen des Eidg, vol. 34. Institutes für Schnee- und Lawinenforschung SLF, 1–223.

Ginzler, C., Hobi, M. L., 2016. Das aktuelle Vegetationshöhenmodell der Schweiz: spezifische Anwendungen im Waldbereich. Schweizerische Zeitschrift für Forstwesen: May/June 2016, Vol. 167, No. 3, 128-135.

Grünewald, T., Bühler, Y., Lehning, M., 2014. Elevation dependency of mountain snow depth. The Cryosphere, 8, 2381-2394.

Hug, M., 2013. Überlebenkünstlerin Alpenerle. Berfgwald Projekt: specht, 2-4.

Höller, P., 2017. Die Bedeutung des Waldes beim Schutz vor Lawinen. In: Schutzwald – Waldwirkungen. Verein der Diplomingenieure der Wildbach- und Lawinenverbauung Österreichs. Heft Nr. 180, 201 p.

Ishikawa, M., Sato, S., Kawaguchi, T., 1969. Snow Density of Avalanche Protection Forest. Journal Jap. Soc. Snow and Ice 31, 14-18. In: Höller, P., 2017. Die Bedeutung des Waldes beim Schutz vor Lawinen. In: Schutzwald – Waldwirkungen. Verein der Diplomingenieure der Wildbach- und Lawinenverbauung Österreichs. Heft Nr. 180, 201 p.

Jamieson,B., Margreth, S., Jones, A., 2008. Application and Limitations of Dynamic Models for Snow Avalanche Hazard Mapping. International Snow Science Workshop 2008 Whistler, 730-739.

Johnson, E. A., 1987. The relative importance of snow avalanche disturbance and thinning on canopy plant populations. Ecology 68, 43-53. In: Brang, P., Schönenberger, W., Ott, E., Gardner, B., 2001. 3: Forests as Protection from Natural Hazards. In: Evans J., 2001. The Forests Handbook. Volume 2. Applying Forest Science for Sustainable Management. Wiley-Blackwell, 816 p.

Jörg, P., Granig, M., Bühler, Y., Schreiber, H., 2012. Comparison of measured and simulated snow avalanche velocities. In: Bründl, M., Margreth, S., 2015. Chapter 9: Intergative Risk Management: The Exmaple of Snow Avalnches. Snow and Ice-Related Hazards, Risks and Disasters, 263-301.

Jørgensen, S. E., 2009. Ecosystem Ecology. 1st ed. Elsevier. Academic Press, 521 p.

Leibundgut, H., 1978. Zur Eröffnung des Seminars über Gebirgswald und Lawinen vom 25. bis 28. September 1978 in Davos. Proceedings IUFRO Seminar Mountain Forests and Avalanches, Davos.

McClung, D. M., 2001. Characteristics of terrain, snow supply and forest cover for avalanche initiation caused by logging. Annals of Glaciology 32, 223-229.

McClung, D., Lied, K., 1987. Statistical and geometrical definition of snow avalanche runout. Cold regions science and technology. Vol 13, 107-119.

McClung, D. M., Schaerer, P., 2006. The Avalanche Handbook, 3rd ed. Mountaineers Books, 342 p.

Omule, S.A.Y., 1984. Fitting Height-Diameter Curves. B.C. Min. For. Research Report RR84008-HQ, 20 p.

Peltola, H., S. Kellom□aki, A. Hassinen, and M. Granander, 2000: Mechanical stability of scots pine, norway spruce and birch: an analysis of tree-pulling experiments in Finland. Forest Ecology and Management, 135 (1), 143-153.

Saeki, M., Matsuoka, H., 1969. Snow-buried young forest trees growing on steep slopes, Seppyo. Japanese Society of Snow and Ice 31, 19–23.

Sampl, P., Granig, M., 2009. Avalanche simulation with SAMOS-AT. International Snow Science Workshop 2009, Davos, Switzerland, pp. 519-523. In: Bründl, M., Margreth, S., 2015. Chapter 9: Intergative Risk Management: The Exmaple of Snow Avalnches. Snow and Ice-Related Hazards, Risks and Disasters, 263-301.

Sappington, J., Longshore, K., and Thomson, D., 2007. Quantifying landscape ruggedness for animal habitat anaysis: a case study using Bighorn Sheep in the Mojave Desert, J. Wildlife Manage., 71, 1419–1426.

Schneebeli, M. and Bebi, P., 2004. Snow and avalanche control. Hydrology, 397-402.

Schweizer, J., Bartelt, P., van Harwijnen, A., 2015. Chapter 12: Snow avalanches. In: Snow and Ice-Related Hazards, Risks and Disasters, 395-436.

Sinickas A., Jamieson, B., 2014. Comparing methods for estimating β points for use in statistical snow avalanche runout models. Cold Regions Science and Technology. Vol. 104-105, 23-32.

Sitko, R., 2008. Využitie geoinformatiky pri identifikácii, hodnotení a rajonizácii funkcií lesa (Utilization of the geoinformatics for the forest functions identification, evaluation and zoning). Dizertačná práca. Zvolen: Technická univerzita vo Zvolene, Lesnícka fakulta, 149 p.

SLF, 2017. Number of avalanche fatalities per year in Switzerland since 1936-1937; WSL Institute for Snow and Avalanche Research SLF.

Sovilla, B., Sonatore, I., Bühler, Y., Margreth, S., 2012. Wet-snow avalanche interaction with deflecting dam: field observations and numerical simulations in a case study. Nat. Hazards Earth Syst. Sci., 12, 1407-1423.

Sterba, H., Marschall, J. and da Silva, A. 1976 Einheitshöhenkurven aus und für Stichprobeninventuren. Allgem. Forstzeitung 87, 349–350.

Techel, F., Zweifel, B. 2013. Recreational avalanche accidents in Switzerland: Trends and patterns with an emphasis on burial, rescue methods and avalanche danger.

International Snow Science Workshop Grenoble – Chamonix Mont-Blanc – 2013, 1106-1112.

Teich, M., Marty, C., Gollut, C., Grêt-Regamey, A., Bebi, P., 2012a. Snow and weather conditions associated with avalanche releases in forests: rare situations with decreasing trends during the last 41 years. Cold Reg. Sci. Technol. Vol. 83-84, 77-88.

Teich, M., Bartelt, P., Grêt-Regamey, A., Bebi, P., 2012b. Snow Avalanches in Forested Terrain: Influence of Forest Parameters, Topography, and Avalanche Characteristics on Runout Distance. Arctic, Antarctic and Alpine Research, Vol. 44, No.4, 509-519.

Teich, M., 2013. Snow avalanches in forested terrain. Dissertation, Department of Civil, Environmental and Geomatic Engineering, ETH, Zürich, Switzerland, 305 p.

Teich, M., Fischer, J.-T., Feistl, T., Bebi, P., Christen, M., Grêt-Regamey, A., 2014. Computational snow avalanche simulation in forested terrain. Natural Hazards and Earth System Science 14 (8), 2233-2248.

UNFCCC, 2001. Report of the conference of the parties. Marrakech, Morocco.

Vacchiano, G., Maggioni, M., Perseghin, G., Motta, R., 2015. Effect of avalanche frequency on forest ecosystem services in spruce-fir mountain forest. Cold Regions Science and Technology 115, 9-21.

Veitinger, J., Sovilla, B., and Purves, R. S., 2014. Influence of snow depth distribution on surface roughness in alpine terrain: a multi-scale approach, The Cryosphere, 8, 547-569.

Veitinger, J. and Sovilla, B., 2016. Linking snow depth to avalanche release area size: measurements from the Vallée de la Sionne field site, Nat. Hazards Earth Syst. Sci., 16, 1953-1965.

Vera Valero, C., Wever, N., Christen, M., Bartelt, P., 2017. Modeling the influence of snowcover temperature and water content on wet snow avalanche runout. Under rewiev for Nat. Hazards and Earth Syst. Sci., 32 p.

Wasem, U., 2005. Auswirkung von Schnee und Lawinen auf junge Bäume. Eidgenössische Forschungsanstalt für Wald, Schnee und Landschaft, WSL. www.waldwissen.net. Online-Version: Stand: 10.02.2005.

6.1 Internet sources

[1] Euforgen – European Forest Genetic Resource Programme, cited on 15.11.2017: http://www.euforgen.org/species/alnus-viridis/

[2] WSL Institute of Snow and Avalanche Research SLF, cited on 5.12. 2017: https://www.slf.ch/en/avalanches/avalanche-warning/avalanche-mapping.html

Appendix

Appendix A

Figure 41: Stillberg 23.4.2008 (SLF).

Figure 42: Stillberg 9.4.2011 (SLF).

Appendix B

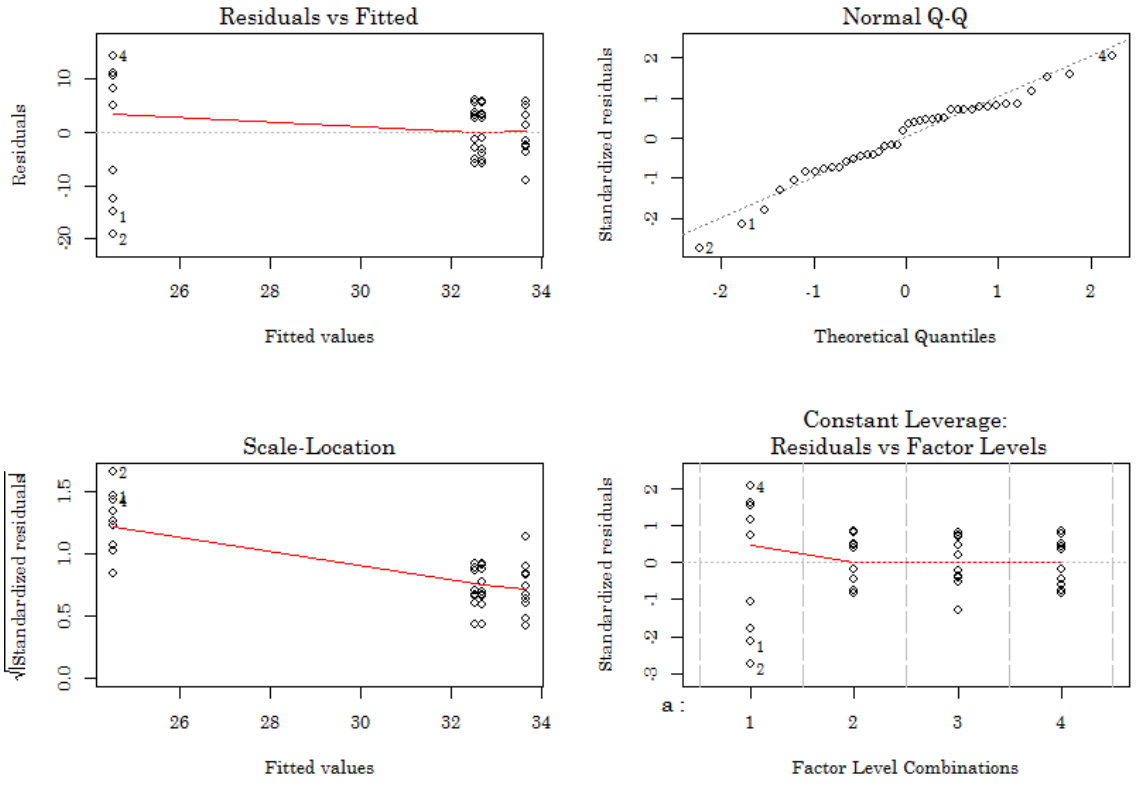

Figure 43: Assumptions for the aov model (from top left): constancy of variance, normality of errors, behaviour of the residuals and influential values for parameter estimates.

List of figures

List of tables

Affirmation

Hereby I assure that I wrote the present master thesis titled

Forest Effects on Avalanche Dynamics: Evaluation and Improvement of the Avalanche Model RAMMS

independently and did not use other than indicated sources. Furthermore, I confirm that I have not submitted this master thesis either nationally or internationally in any form.

Innsbruck, 04/2018

Natalie Brožová